University of California
Los Angeles

Theory of Quantum Oscillations in Cuprate Superconductors

A dissertation submitted in partial satisfaction
of the requirements for the degree
Doctor of Philosophy in Physics

by

Jonghyoun Eun

2012

Abstract of the Dissertation

Theory of Quantum Oscillations in Cuprate Superconductors

by

Jonghyoun Eun

Doctor of Philosophy in Physics

University of California, Los Angeles, 2012

Professor Sudip Chakravarty, Chair

Cuprate supercoductors show pseudogap state below its transition temperature T^*. The pseudogap state is distinct from superconducting state(critical temperature $T_c < T^*$). Two states may coexist and superconductivity developes from the pseudogap state which can be explained by commensurate and incommensurate d-density wave (dDW) orders. Quantum oscillations help us to understand the pseudogap state. Hall coefficient, magnetization, conductance and specific heat oscillate as a function of external field in $YBa_2Cu_3O_{6+\delta}$ (YBCO), $Nd_{2-x}Ce_xCuO_4$ (NCCO) and other cuprates. The oscillation frequency F is proportional to the area of closed-orbits in reconstructed Fermi surface. High magnetic field for quantum oscillation experiment suppresses superconductivity. Therefore, quantum oscillations measure reconstructed Fermi surface of pseudogap state.

Electron-doped cuprate superconductor NCCO shows only hole pocket frequency peak. Experimental results can be explained by period-2 dDW order and white-noise disorder. Disorder in the system removes electron pocket frequency and adjusts the amount of magnetic breakdown effect corresponding to very high frequency. Period-8 density wave order can explain quantum oscillations in the pseudogap state of hole-doped $YBCO$. Only electron pocket frequency is observed. Period-8 dDW order generates small but many hole pockets in the reconstructed Fermi surface. Small hole pocket frequency is too slow to be observed.

The dissertation of Jonghyoun Eun is approved.

Thomas M. Liggett

Yaroslav Tserkovnyak

Joesph Rudnick

Sudip Chakravarty, Committee Chair

University of California, Los Angeles

2012

To my parents and fiancée . . .

Table of Contents

List of Figures

Acknowledgments

There are a number of people who have been supporting me in many respects for last six years. Without their help this dissertation would not be made ever.

First, I thank my academic advisor, Dr. Sudip Chakravarty. He has been supporting me in both academic and emotional respects. He has helped my transition from a student to a researcher. He is an extremely good research supervisor in our research group and an incredibly excellent lecturer in a class. Besides, he was concerned on my teaching skill; it was my *golden age* in my teaching experience when I was a disccusion TA for his undergraduate quantum mechanics courses. I learned how to present brilliant but abstract ideas to students and how to interact with my students under his supervisory. Also he tuaght me academic writing in physics. He coauthored and wrote my research papers and revised all of my writings. I cannot acknowledge all of his effort on me enough in this short space.

I was fortunate to work and discuss with distinguished faculty members in the department of physic and the department of mathematics at UCLA. I thank Dr. Joseph Rudnick, Dr. Yaroslav Tserkovnyak, Dr. Alexander Levine, and Dr. Thomas Liggett for their helpful discussion and great lectures. In addition, I thank the Institute for Digital Research and Education(IDRE) at UCLA for the technical and instrumental assistance. Without IRDE, I could not run my simulation codes on their Hoffman2 cluster computer.

Other than my advisor Dr. Chakravarty, many collaborators helped me to finish my research papers and this dissertation. I would like to acknowledge Dr. Xun Jia and Zhiqiang Wang in our research group. I also thank Dr. Pallab Goswami, Dr. David Schwab, Dr. David Garcia-Aldea, Koji Sato and Chen-Hsuan Hsu for their discussion of condensed matter physics. I appreciate Dr. Jiyong Park and Hanjun Kim for their discussion on numerical methods. Without them, I could not finish my numerical analysis. This dissertation is based on my research papers, two of which are published on jornals of the American Physical Society. The last paper is about to be submitted.

My best man of wedding, Albert (Yubo) Kao has been helping me for everything from

my first day in UCLA. And I have so many wonderful friends who have helped me a lot in every respect. Their support tremendously helped me to complete my Ph.D. degree. To all of them I would like to show my sincere appreciation. I cannot list all of their names; there are too many. My fiancée, Seungjoo Hwang has been helping me in all aspects. I cannot thank her enough for everything. My parents, Dr. Seyun Eun and Dr. Hei Sun Han have been the greatest support for me ever since I was born. My attitude and passion toward research are inherited from and tauhgt by my parents. The largest portion of my Ph.D. degree is owed to them. I wish I could express how much I am grateful for my parents and my fiancée for everything but words can never fully express the heart.

Jonghyoun Eun

April, 2012

Los Angeles, California

Vita

1981	Born, Seoul, The Republic of Korea.
2006	B.S. in Physics, Seoul National University, Seoul, The Republic of Korea
2008–Present	Research Assistant, Theoretical Condensed Matter Research Group, Department of Physics and Astronomy, University of California, Los Angeles, California, USA.

Publications

Quantum oscillations in electron-doped high-temperature superconductors
(Phys. Rev. B 82, 094515), 2010.
Magnetic breakdown and quantum oscillations in electron-doped high-temperature superconductor $Nd_{2-x}Ce_xCuO_4$
(Phys. Rev. B 84, 094506), 2011.
Quantum oscillations in $YBa_2Cu_3O_{6+\delta}$ *from an incommensurate d-density wave order*
(To be published).

CHAPTER 1

Introduction

1.1 High Temperature Cuprate Superconductors

Discovery of superconductivity in mercury below $\sim 4\ K$ by Heike K. Onnes in 1911 has attracted humongous attention to condensed matter physicists. Besides mercury, aluminum, lead, zinc and other elements reveal their superconductivity at low temperature below $5K$. Some conventional superconductors are type-I superconductor in which the expulsion of external magnetic field from a superconductor (Meissner effect) disappears only when field is large enough. Superconductivity exists only below *critical temprature* T_c, which is typically in the order of $O(K)$ for most of convenctional superconductors. Among conventional superconductors, magnesium diboride (MgB_2) discovered by Nagamatsue and collaborators in 2001 has the highest critical temperature($T_c = 39\ K$).

In 1957, convincing explanation about conventional superconductor was introduced by Bardeen, Cooper, and Schrieffer.[1] Their explanation is named *BCS* theory which assumes that two electrons form a Cooper pair by attraction between electrons stronger than the Coulomb repulsion. In most conventional superconductors, this attraction indirectly arises from the coupling of electrons to the crystal lattice; one electron deforms the lattice, then the other electron interacts with it. The interaction between two electrons via the lattice deformation lead to BCS ground state seprated from excited states by an energy gap. This energy gap is responsible for many feaures of BCS superconductors such as critical field, specific heat, and electromagnetic properties arise. Attraction between electrons is also known as superconducting pairing order, which is believed to be the core mechanism

of superconductivity and dissipationless current carrying. Conventional superconductor is also known as s-wave superconductor since superconducting pairing order has spherically symmetric s-wave orbital function; in contrast, unconventional superconductors (explained below) have asymmetric pairing order. The fact that two electrons of a Cooper-pair are not distinguishable enforces total wavefunction of a Cooper-pair to be anti-symmetric. Since spin singlet Cooper-pair has anti-symmetric spin fuction, it can have only even orbital angular momentum number: $l = 0, 2, 4 ...$

BCS theory was challenged since unconventional high temperature superconductor was discovered. *Unconventional* superconductor means it does not conform to BCS theory mentioned above; orbital function of a Cooper pair is not s-wave. Neither is superconducting pairing order originating from electron-phonon channel. The origin of superconducting order is not well-kown but its anisotropy in momentum space leads us to believe that it is different from BCS type s-wave pairing order. The nomenclature *high-T_c* is introduced because most unconventional superconductor shows superconductivity at higher temperature than conventional s-wave superconductor; the first high-T_c ($\sim 30K$) superconductor $LaBaCuO$ was discovered in 1986 by IBM researchers Muller and Bednorz. It has higher T_c than most of conventional superconductor by one order of magnitude; later, superconductors with even higher T_c are discovered: Thallium barium calcium copper oxide($Tl_2Ba_2Ca_2Cu_3O_{10}$) with $T_c = 125K$ in 1988 and Mercury barium calcium copper oxide($HgBa_2Ca_{m-1}Cu_mO_{2m+2+\delta}$) in 1993. Many high T_c superconductors contain copper-oxide and they are named cuprate. Superconductivity in this cuprate superconductor arises from Mott insulating phase; which is insulator with *Mottness* such as twice sign changes of the Hall coefficient as electron doping per site increases from $n = 0$ to $n =2$ and a pseudogap away from half-filling $n = 1$. Of course there is a superconductor which is neither convenctional BCS superconductor nor cuprate superconductor; iron-arsenide superconductor is discovered and studied relative recently, in 2008. Still, its T_c (at most $\sim 50K$) is below that of cuprate and many physical properties are to be determined by further experiments. Present thesis shall discuss cuprate unconventional superconductor which has abundant experimental features.

Cuprate superconductor has anisotropic d-wave superconducting order, i.e. orbital angular momentum of the Cooper-pair $l = 2$. This d-wave orbital angular momentum of electron-electron pairing order can be verified by superconducting quantum interference device (SQUID) measurement of Josephson current through a junction between BCS superconductor and cuprate superconductor. Since the Josephson current is proportional to amplitudes of both BCS type and unconventional superconducting orders, the angular dependence of unconventional cuprate superconducting order is detected by measuring the Josephson current with different shapes of junction. [2] d-wave orbital function is anisotropic and it is also implicated by the power-law dependence of the nuclear magnetic resonance (NMR) relaxation rate and the specific heat capacity on temperature.

Research on high-T_c superconductors has revealed that there exist combinations of different pairing orders, which are competing with one another. [3] Those competing orders are different types of broken symmetries such as rotational and translational symmetries which, in turn, make phase diagram of cuprate complicated. Phase diagram of superconductor usually has two axes: charge carrier doping and temperature. At low doping level, three dimensional antiferromagnetic order (AF) exists below its transition temperature T_N. As more charge carriers are doped on the superconductor sample, superconductivity arises at low temperature below the critical temperatures depending on its doping. It has the highest critical temperature(T_c) at *optimal doping*. And superconductivity persists around the optimal doping. This regime in phase diagram is called superconducting dome. In its low doping part system behaves under the influence of the parent Mott insulator. And it is believed that there exists another dome of normal state with a certain order which is competing with superconductivity; it is called pseudogap pairing order, which exists below its transition temperature T^* ($> T_c$) and around or less than the optimal doping. Superconducting dome and pseudogap dome are not necessarily coinciding. Still, there is overlapping regime between those two domes where superconducting pairing order and pseudogap order are competing but superconducting order is dominant. Since this pseudogap exists even without superconductivity, it was believed to be some *exotic* non-Fermi liquid state. But

experiments of quantum oscillations (explained in the following section) propose that the pseudogap phase is Fermi liquid state; it is resided by electron- and hole-like quasiparticles in a reconstructed Fermi surface. Intersections and boundaries of three phases (antiferromagnetism, superconducting state, and pseudogap state) are quantum critical points which yeild very complicated phase diagram of cuprate superconductor. (See figure 1.1)

In order to deeply understand this d-wave superconducting order, many research groups study the pseudogap state where superconductivity is totally suppressed; but superconductivity seems to arise from pseudogap state and sometimes coexists with it. The suppression of superconductivity is obtained by applying high magnetic field, $35T$ or above. Even though it is very high field range, it has merely minimal impact on the system in the view of energetics except suppression of superconductivity; energy level of $35T$ is equivalent to $35K$ which is below the Fermi energy level so that it is not a big perturbation for the system. Cuprate superconductors in high magnetic field reveal normal state(pseudogap state) from which superconductivity developed as external field is lowered. Therefore, the main concern of present thesis will be the pseudogap state of cuprate superconductor. Quantum oscillation measurements can achieve this goal. It will be discussed in the following sections.

1.2 Quantum Oscillations

Quantum oscillations of conductance (*Shubnikov-de Haas oscillation*), magnetization (*de Haas-van Alphen oscillation*), specific heat, and Hall coefficient have been widely studied in order to understand the pseudogap state. In this respect, quantum oscillation experiments are performed at high fields 35-65T and low temperatures; this amount of external field will not energetically perturb the system but will suppress superconductivity and leave the pseudogap order. In the present section, general argument about quantum oscillation is given and details on quantum oscillation in cuprate superconductors are covered in the following sections.

Quantum oscillation of physical quantities such as conductance, magnetization, specific

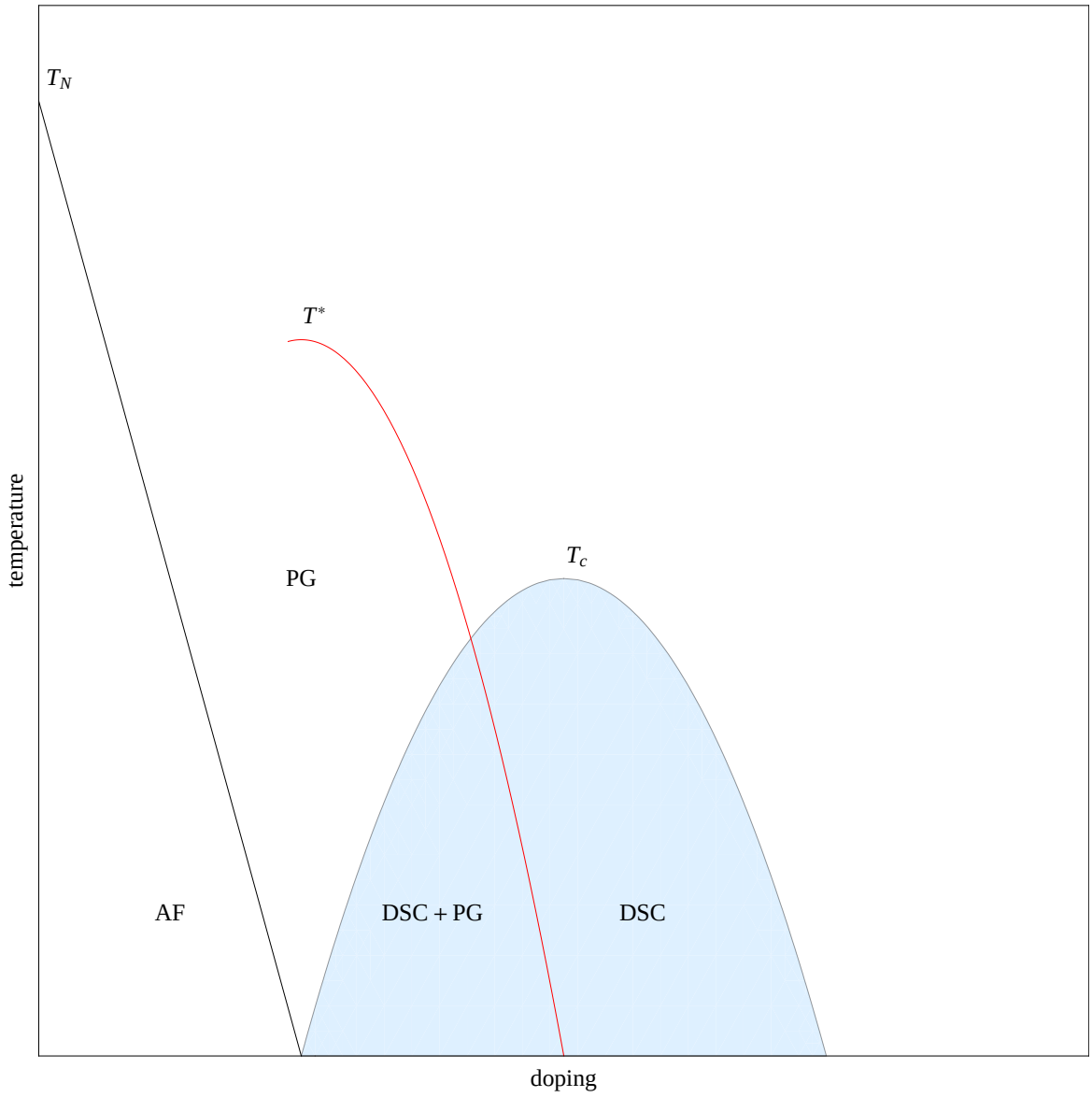

Figure 1.1: Schematic phase diagram of cuprate superconductors. Four phases are marked: antiferromagnetism(AF), Pseudogap state(PG), d-density superconducting state(DSC). Entire region painted light blue is superconducting state and red curve surrounds pseudogap state. In the intersection between red and light blue regions, superconducting order and normal state coexists.

heat, and Hall coefficient is due to periodicity of the Landau levels. Energy of each Landau level is:

$$\epsilon_n = \hbar\omega_c(n + \frac{1}{2}) \tag{1.1}$$

whre ω_c is a cyclotron frequency $\frac{eB}{mc}$. Here B is external magnetic field, e is electron charge, m is mass of electron, and c is the speed of light. As the external field B increases, energy level of quantized orbits (Landau levels) pass thorough the Fermi level periodically. This periodicity leads to the Onsager formula for the frequency of the quantum oscillations

$$F = \frac{\hbar c}{2\pi e} A(\epsilon_F) \tag{1.2}$$

where $\hbar$ is Plank constant and ϵ_F is Fermi energy level. And this periodicity does not necessarily mean that quantum oscillations have a sinusoidal wave form. Within the two dimensional Fermi liquid theory, spectral function is a sum over δ-functions:

$$A(\epsilon) = 2\frac{eBL_xL_y}{2\pi\hbar c} \sum_n \delta(\epsilon - (n + \frac{1}{2})\hbar\omega_c) \tag{1.3}$$

where L_x and L_y represent system size in two dimension. Therefore, Landau levels are series of spikes as a function of energy, which in turn leads to the *non*-sinusoidal wave form of quantum oscillations as a function of magnetic field. In the framework of the Lifshitz-Kosevich theory, the field-dependent oscillatory part of physical quantities such as conductance and magnetization for two dimensional Fermi surface is expressed as sum over sinusoidal functions. Dingle damping factor(D_p) is present to include disorder in the system and Lifshitz-Kosevich theory of quantum oscillations is:

$$\tau_{oscillatory} \sim \sum_p R_p D_p \cos[2\pi p(\frac{F}{B} - \frac{1}{2}) \pm \frac{\pi}{4}] \tag{1.4}$$

where p is the index(order) of harmonics, F is frequency given by equation 1.2, k is Boltzmann constant, T is temperature, B is external field, and R_p is $\frac{4\pi^2 kTp}{\hbar\omega_c}\sinh(\frac{2\pi^2 kTp}{\hbar\omega_c})$.[4] And the Dingle factor is $D_p = exp(-\frac{p\pi}{\omega_c\tau})$ where τ is scattering time, or mean-free time.

According to above equation 1.4, the larger charge carrier orbit is, the more vulnerable to disorder; if we suppose that mean free path l is the same for both the smaller and the larger

orbits, which is not an unreasonable assumption. D_p can explain the effect of disorder as follow. With band structure and electron-hole pairing order (to be explained in the following section), charge carrier orbits formed due to external magnetic field is not circular but just closed contour as shown in figure 1.2. But the wave number at the Fermi level k_F can be estimated by assuming that those charge carrier orbits are circular: area of a charge carrier orbit in momentum space $A = \pi k_F^2$. Then, scattering time τ is successively calculated from k_F by $l = v_F\tau$ and $m^* v_F = \hbar k_F$; it yields $\tau = \frac{m^* l}{\hbar k_F}$. With this equation, τ becomes shorter for the larger area A as long as mean free path l is the same for both orbits. Then, the Dingle factor vanishes for very small τ i.e. the larger Fermi surface area(A). One also note that cyclotron mass m^* is not the mass of electron; instead m^* is calculated from the second derivative of energy as a function of momentum.

Infinite series of sinusoidal functions in equation 1.4 is not necessarily sinusoidal as mentioned above; with sufficiently high disorder level Dingle damping factor D_p for $p \geq 2$ all vanishes therefore, only the first term of equation 1.4 survives and the oscillation becomes sinusoidal. This is why quantum oscillations measured in experiments show sinusoidal wave forms. Arguements about quantum oscillations above are generally applied to both Shubnikov-de Haas (S-dH) oscillation and de Haas-van Alphen oscillation.

Other than removal of the larger pockets in S-dH oscillation, disorder has another role in quantum oscillations. Surely, *any* amount of disorder breaks translational symmetry. But a moderate intensity of disorder can be understood in terms of a self-consistent Born approximation.[5] Due to the effect of disorder, Landau levels are broadened and δ-functions in equation 1.3 are replaced by functions with less sharp peaks such as Lorentzian function. Since disorder slows down quasi-particles in the sample, it takes more time for a quasi-particle to complete its orbit (pocket). Consequently, frequencies of quantum oscillations decrease; so does energy ϵ of closed-orbits in Fermi surface. This downward energy shift is:

$$\Delta(\epsilon) = \frac{1}{\pi} P \int d\omega \frac{\Gamma(\epsilon, \omega)}{\epsilon - \omega} \tag{1.5}$$

where $\Gamma(\epsilon, \omega) = \pi \sum_{k \neq k'} |V_{k,k'}|^2$ and $\epsilon_k = \epsilon_F = \epsilon$. [3] But frequency shift due to disorder is

small enough that quantum oscillation frequency does not change much with disorder level.

Pronounced oscillation of Hall coefficient as a function of magnetic field H indicates that two types of charge carrier form their own closed orbits: electron and hole. A closed orbit of charge carrier in Fermi surface is also known as a *pocket*. Simply Hall resistivity for a single electron (or hole) pocket is $\frac{1}{nec}$ within a conventional Fermi liquid theory. Here n is charge carrier density. And it is known that the combined Hall coefficient R_H for two different types of charge carriers:

$$R_H \approx \frac{R_{electron}\sigma_{electron}^2 + R_{hole}\sigma_{hole}^2}{(\sigma_{electron} + \sigma_{hole})^2} \tag{1.6}$$

where R_i and σ_i are the individual Hall coefficients and the conductivities of electron and hole pocket respectively. If there is only one type of charge carriers (either electron- or hole-pocket), scattering rates from the numerator and the denominator cancel out each other and no oscillation in Hall coefficient is present. But with two types of charge carriers (both electron and hole), R_H oscillation arises from those of electron- and hole-conductivities in equation 1.6.

1.3 Interpretation of Quantum Oscillations

It is challenging to understand the pseudogap state. Only one frequency peak corresponding to single closed orbit of electron (electron pocket) is observed from quantum oscillations in electron-doped superconductor $Nd_{2-x}Ce_xCuO_4$ (NCCO). And hole-doped superconductor $YBa_2Cu_3O_{6+\delta}$ (YBCO) shows only electron pocket frequency. But oscillation of Hall coefficient is an evidence for the existence of two closed pockets, which conflicts with the single frequency peak of quantum oscillations. A short answer to this mystery can be that the Dingle factor removes quantum oscillations as in 1.4. As explained in the previous section, the larger pocket in the Fermi surface is exponentially more vulnerable to disorder. Thus, the larger pocket in Fermi surface is unseen in quantum oscillation experiments; since disorder is inevitably combined in real experiments. This may answer why electron-pockets (hole-pockets) are unseen in electron-doped (hole-doped) superconductor from quantum os-

cillation measurements. But too much disorder also wipes out the smaller pockets and no frequency peaks would appear. Of course, too small amount of disorder is not enough to suppress oscillation frequency from the large pockets. This crucial role of disorder is again pointed out in the following sections.

An exact transfer matrix method along with the Pichard-Landauer formula[6],[7] for the conductance enables us to numerically calculate conductance oscillation as a function of external magnetic field. Simulation of S-dH oscillations helps us to understand pseudogap order (which is often called particle-hole pairing order) and the role of disorder.

For the transfer matrix calculation, Hartree-Fock mean field Hamiltonian in coordinate space is used. Band structure of tight-binding model describes kinetic term of electrons as hopping between lattice points of quasi-one-dimensional (quasi-1D) lattice($N \times M$ and $N \gg M$). Hopping terms are written in terms of fermionic creation and annihilation operators:

$$H_{hopping} = \sum_{\mathbf{r} \neq \mathbf{r}'} t_{\mathbf{r},\mathbf{r}'} c^{\dagger}_{\mathbf{r}} c_{\mathbf{r}'} + h.c. \tag{1.7}$$

And the electron-electron interaction introduces a particle-hole pairing order term. Full Hamiltonian is involved with four fermionic operators to express electron-electron interaction; in the mean field theory, two of them are replaced by the average amplitude as below.

$$H_{interaction} = \sum_{\mathbf{r},\mathbf{r}',\mathbf{l},\mathbf{l}'} V_{\mathbf{r},\mathbf{r}',\mathbf{l},\mathbf{l}'} c^{\dagger}_{\mathbf{r}} c^{\dagger}_{\mathbf{r}'} c_{\mathbf{l}} c_{\mathbf{l}'} \rightarrow \sum_{\mathbf{r},\mathbf{r}'} \tilde{V}_{\mathbf{r},\mathbf{r}'} c^{\dagger}_{\mathbf{r}} c_{\mathbf{r}'} + h.c. \tag{1.8}$$

As a candidate for this particle-hole pairing order($\tilde{V}_{\mathbf{r},\mathbf{r}'}$), several different density wave orders are discussed in the following sections. Then, the mean field Hamiltonian for the transfer matrix method is obtained by combining above two equations. For the case of d-density wave (dDW) order, Hamiltonian is

$$H_{dDW} = \sum_{\mathbf{r}} \epsilon_{\mathbf{r}} c^{\dagger}_{\mathbf{r}} c_{\mathbf{r}} + \sum_{\mathbf{r} \neq \mathbf{r}'} t_{\mathbf{r},\mathbf{r}'} \ \mathrm{e}^{i a_{\mathbf{r},\mathbf{r}'}} c^{\dagger}_{\mathbf{r}} c_{\mathbf{r}'} + h.c. \tag{1.9}$$

The first term $\epsilon_{\mathbf{r}}$ is onsite energy. It includes onsite disorder(see below) and spin-density wave order $V_S \sigma_z$ if exists. A constant perpendicular magnetic field B is included via the Peierls phase factor $a_{\mathbf{r},\mathbf{r}'} = \frac{2\pi e}{h} \int_{\mathbf{r}'}^{\mathbf{r}} \mathbf{A} \cdot \mathrm{d}\mathbf{l}$, where $\mathbf{A} = (0, -Bx, 0)$ is the vector potential in

the Landau gauge. And $t_{\mathbf{r},\mathbf{r}'}$ consists of both hopping term and dDW order. For the nearest neighbor terms, it is

$$\begin{aligned} t_{\mathbf{r},\mathbf{r}+\hat{\mathbf{x}}} &= -t + \tfrac{iW_0}{4}(-1)^{\frac{r_x}{a}+\frac{r_y}{a}}, \\ t_{\mathbf{r},\mathbf{r}+\hat{\mathbf{y}}} &= -t - \tfrac{iW_0}{4}(-1)^{\frac{r_x}{a}+\frac{r_y}{a}}, \end{aligned} \tag{1.10}$$

where W_0 is the amount of dDW order parameter and a is a lattice spacing.

We consider a quasi-1D system, $N \gg M$, with a periodic boundary condition along y-direction; N is $10^5 \sim 10^6$ and the width M is $30 \sim 128$. When the amplitudes on the slice n for an eigenstate with a given energy is

$$\Psi_n = (\psi_{n,1}, \psi_{n,2}, \ldots, \psi_{n,M})^T, \tag{1.11}$$

then the amplitudes on three successive slices satisfy the relation below

$$\begin{bmatrix} \Psi_{n+1} \\ \Psi_n \end{bmatrix} = \begin{bmatrix} T_n^{-1}A_n & -T_n^{-1}B_n \\ 1 & 0 \end{bmatrix} \begin{bmatrix} \Psi_n \\ \Psi_{n-1} \end{bmatrix} = \mathbf{T}_n \begin{bmatrix} \Psi_n \\ \Psi_{n-1} \end{bmatrix} \tag{1.12}$$

where T_n, A_n, and B_n are $M \times M$ matrices. They are derived from Schrodinger equation $H_{dDW}\Psi_n = \mu\Psi_n$ where μ is the chemical potential energy. Then, the left handed-side of the Schrodinger equation becomes $T_n\Psi_{n+1} + A'_n\Psi_n + B_n\Psi_{n-1}$ by fermionic creation and annihilation operators of H_{dDW}. This yields the final equation $T_n\Psi_{n+1} = A_n\Psi_n - B_n\Psi_{n-1}$ with $A_n = \mu - A'_n$. And it is the first row of above matrix equation.

Next step is calculating 2M Lyapunov exponents, γ_i, of $\lim_{N\to\infty}(\mathbb{T}_N^\dagger\mathbb{T}_N)$, where $\mathbb{T}_N = \prod_{j=1}^{j=N}\mathbf{T}_j$, are defined by the corresponding eigenvalues $\lambda_i = e^{\gamma_i}$. All Lyapunov exponents $\gamma_1 > \gamma_2 > \ldots > \gamma_{2M}$, are computed by a procedure given in Ref. [8]. The Pichard-Landauer formula

$$\sigma_{xx}(B) = \frac{e^2}{h}\mathrm{Tr}\sum_{j=1}^{2M}\frac{2}{(\mathbb{T}_N\mathbb{T}_N^\dagger) + (\mathbb{T}_N\mathbb{T}_N^\dagger)^{-1} + 2}, \tag{1.13}$$

gives us the longitudinal conductance.

For spin-density wave, the generalization is straightforward; the term W_0 will be absent. And the diagonal term $\epsilon_{\mathbf{r}}$ in equation 1.9 is modified to include spin-density wave order $V_S\sigma_z$. Now spin up and down states are distinct, therefore, equation 1.11 becomes

$$\Psi_n = (\psi_{n,1,\uparrow}, \ldots, \psi_{n,M,\uparrow}, \psi_{n,1,\downarrow}, \ldots, \psi_{n,M,\downarrow})^T. \tag{1.14}$$

Consequently, T_n, A_n, and B_n are replaced by larger $2M \times 2M$ matrices: $\tilde{T}_n$, $\tilde{A}_n$, and $\tilde{B}_n$. $\tilde{A}_n$ reflects the spin-dependence of $\epsilon_{\mathbf{r}}$:

$$\tilde{A}_n = \begin{bmatrix} A_{n,\uparrow} & 0 \\ 0 & A_{n,\downarrow} \end{bmatrix} \tag{1.15}$$

And $\tilde{T}_n$ is simply

$$\tilde{T}_n = \begin{bmatrix} T_n & 0 \\ 0 & T_n \end{bmatrix}. \tag{1.16}$$

$\tilde{B}_n$ is similarly extended. As above extended *tilde* matrices are block-diagonal because there is no spin-flipping term in the Hamiltonian.

Last but not least, disorder is introduced; this onsite disorder plays an important role in controlling magnetic breakdown across different bands as mentioned in the previous section. The effect of disorder can be imposed by adding random variable to the transfer matrix element $\epsilon_{\mathbf{r}}$ in equation 1.9. While doing numerical simulation, type and amplitude of disorder were smartly tuned in order to reproduce quantum oscillation signature consistent with experiments. As described above, disorder can be one of the keys to resolve the discrepancy between s-dH oscillation measurement and the Hall coefficient measurement. Also the amount of magnetic breakdown across two orbits in Fermi surface is adjusted by disorder level. At low disorder level, combinations of electron($F_{electron}$) and hole(F_{hole}) pocket frequencies are measured: $F_{electron} \pm F_{hole}$. Moreover, the second harmonics and the third harmonics (twice or triple frequency of the original electron/hole pocket frequency given by equation 1.2) are observed; they are respectively corresponding to $p = 2$ and $p = 3$ terms in equation 1.4. This magnetic breakdown effect has a crucial role in explaining very high frequency S-dH oscillation of NCCO sample in section 1.4.1. In the successive sections, more details of quantum oscillations in NCCO and YBCO are given in the contexts of the exact transfer matrix method and the role of disorder.

1.4 Electron-doped

$Nd_{2-x}Ce_xCuO_4$ ($NCCO$) is electron-doped cuprate superconductor. Period-2 (commensurate) d-density wave order yields a viable explanation for quantum oscillations of $NCCO$. Series of experiments [9],[10],[11] can be understood in the context of tight binding model and commensurate d-density wave pairing order.

In chapter 2, ab-plane longitudinal conductance σ_{xx} as a function of magnetic field is calculated by transfer matrix method(see section 1.3). In experiments, c-plane resistivity(ρ_c) is measured. It is larger than ab-plane resistivity by factor of 10^5 but oscillatory parts of both resistivities are similar. Therefore, numerical calculation of σ_{xx} reflects experimental behavior of ρ_c. More rigorous argument is given in Chapter 3.

This σ_{xx} calculation helps us to understand the first experiment [9]. Not only d-density wave but also spin density wave is considered as a particle-hole pairing order, $\tilde{V}_{\mathbf{r},\mathbf{r}'}$ in equation 1.8. White noise disorder was tuned in order to suppress other frequency peaks except one peak(F_{hole} <$300T$). Only slow frequency peak corresponding to a small hole pocket is observed in the experiment; a large electron pocket is unseen. Later experiment of Shubnikov-de Haas (S-dH) oscillation in $Nd_{2-x}Ce_xCuO_4$ (NCCO) indicates a very high frequency peak ($\sim 10kT$) as well as a low frequency peak(F_{hole}).[10][11]

The measurements in NCCO for 15%, 16%, and 17% doping level are of our interest. There are more features to be noticed as follows. First, conductance is measured under the magnetic field in the range of 30-64T. This is far above the upper critical field of NCCO which is believed to be about $10T$ or less. Beyond the upper critical field, superconductivity is totally destroyed so that we can interpret quantum oscillations in the context of the pseudogap state that is *not* associated with the vortex state of superconductors. Thus, vortices are not considered in NCCO problems. Two-fold commensurate particle-hole pairing order such as d-density wave or spin-density wave is enough to pursue Shubnikov-de Haas oscillations in NCCO.

As the doping level x increases, features of quantum oscillations also change reflecting

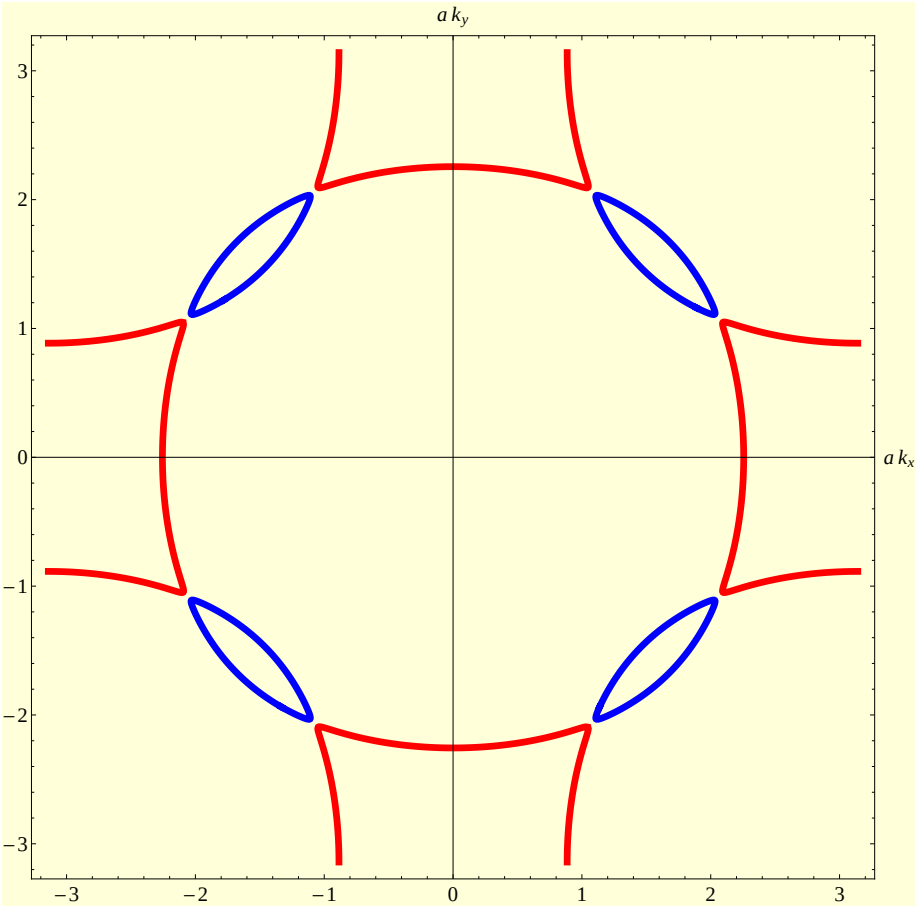

Figure 1.2: Fermi surface in the full Brillouin zone of NCCO with $x = 0.15$ doping.

topology of Fermi surface. Especially, from $x = 0.16$ to $x = 0.17$ frequency of S-dH oscillations drastically jumps from $280T$ at $x = 0.16$ to 10.7 kT at x =0.17.[9] This jump of S-dH oscillation frequency indicates a transformation of the Fermi surface (see figure 1.2 and 1.3); High frequency of quantum oscillation arising at $x = 0.17$ is corresponding to a *quite large* hole pocket from *un*-reconstructed Fermi surface. Namely, quantum phase transition occurs at $x = 0.17$.[10],[11],[12]

The experiment of S-dH oscillation is numerically simulated by transfer matrix method discussed in the section 1.3. In the numerical calculation, two types of particle-hole pairing order are considered; and the amplitude of pairing order is tuned for different doping levels. In particular, the amplitude is chosen to be zero at $x = 0.17$ where phase transition occurs

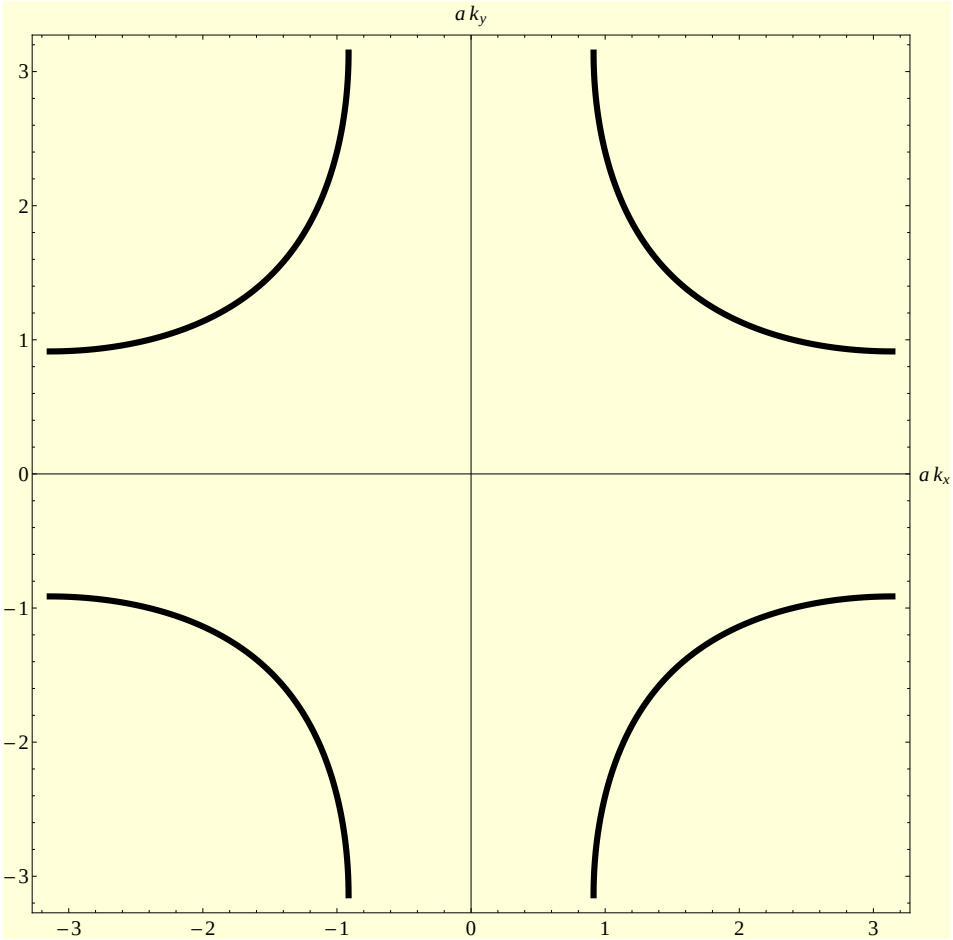

Figure 1.3: Fermi surface in the full Brillouin zone of NCCO with $x = 0.17$ doping.

as described above. Along with the pairing order amplitude, disorder plays an important role; without disorder, it is impossible to explain why slow oscillations frequency F_{hole} with doping $x = 0.15$-0.16 vanishes below $30T$. This damping arises from the Dingle factor $D_p = exp(-\frac{p\pi}{\omega_c \tau})$ from equation 1.4; at low external field, exponent of Dingle factor D_p goes to negative infinity so that Dingle factor becomes zero. Similarly, for doping $x = 0.17$ oscillations are wiped out below $60T$.

As mentioned above, *a certain* symmetry is broken when doping x is below 0.17 but it is controversial what the broken symmetry is. Thus, d-density wave order and spin density wave order are chosen to calculate S-dH oscillations for doping $x = 0.15$ and 0.16. Both density wave orders reproduce experiments well; single slow frequency (F_{hole}) smaller than $300T$ corresponding to hole pockets is calculated by transfer matrix method with proper amount of disorder. Medium frequency ($F_{electron}$) around $2000T$ corresponding to electron pockets appears with less amount of disorder. At *very* low disorder level, magnetic breakdown across electron- and hole-pockets occurs; and combination frequency such as $F_{electron} \pm F_{hole}$ is observed. This magnetic breakdown effect is discussed more in the following subsection 1.4.1. Naturally, too much disorder wipes out all the frequencies. At doping $x = 0.17$, high frequency corresponding to one big hole pocket *without* Fermi surface reconstruction is calculated by setting pairing order zero as mentioned above. This transfer matrix calculation shows that some types of pairing order combined with proper amount of disorder explain experiments well.

1.4.1 Magnetic breakdown Effects

Very high frequency peak around $10kT$ of Shubnikov-de Haas (S-dH) oscillation in $Nd_{2-x}Ce_xCuO_4$ (NCCO) is observed other than low frequency (F_{hole} <$300T$) and high frequency($F_{electron}$ ~$2000T$) erased by disorder.[10],[11] The origin of the very high frequency peak is the magnetic breakdown between electron- and hole pockets across small energy gaps in reconstructed Fermi surface due to two-fold commensurate d-density wave order. Since spin density wave order does not give a distinct result compared to d-density wave order

as described above, only d-density wave order is considered for magnetic breakdown effect of NCCO. Again, disorder intensity is a key player as to tuning the amount of magnetic breakdown. At low disorder intensity, too many magnetic breakdown effects exist according to numerical calculation of S-dH oscillation. On the other hand, too much disorder removes *all* the magnetic breakdown effects, which is inconsistent with the experiment.

Figure 1.4 is *reconstructed* Fermi surface with smaller pairing order compared to figure 1.2. From the figure, the electron pocket marked with black arrows explains why electron pockets are unseen; along the orbit of the electron pocket, momentum of quasi-particle changes a lot whenever the quasi-particle reflects at the junctions. This large change in the momentum of quasi-particle makes it less probable that the quasi-particle goes around the orbit and forms a closed-orbit. This is why electron pockets with *sharp* points are unseen by S-dH oscillation measurements. Hole pocket depicted as red and blue dashed curves in the figure also has sharp junctions. But it has only two such points rather than four junctions along the electron pocket; less number of sharp junctions explains the presence of hole pocket frequency. Very high frequency ($\sim 10^4 T$) is corresponding to the orbit of red dashed and solid curve (the large magnetic breakdown orbit mentioned above). As a matter of fact, this orbit consists of four electron pockets and four hole pockets and it is involved with eight times of tunneling effect from electron pocket to hole pocket and vice versa. The magnetic breakdown orbit is more vivid than electron pocket because change of quasi-particle momentum before and after the magnetic breakdown (tunneling) is smaller.

The argument about vulnerability of pocket (orbit) proportional to its area in Fermi surface is still valid. At high disorder level, very high frequency corresponding to the red orbit in figure 1.4 vanishes before the hole pocket with smaller area. If extra attention is paid to the orbit consisting of blue and red *solid* curve (looking like *8*), quasi-particles along this trajectory experience two reflection within electron pockets and twelve tunnelings between hole and electron pockets. This *super*-frequency orbit is of course more unstable than the red orbit with very high frequency but this super-frequency ($\sim 2 \times 10^4 T$) is still shown in the transfer matrix calculation for S-dH oscillations; at very low disorder level. But electron

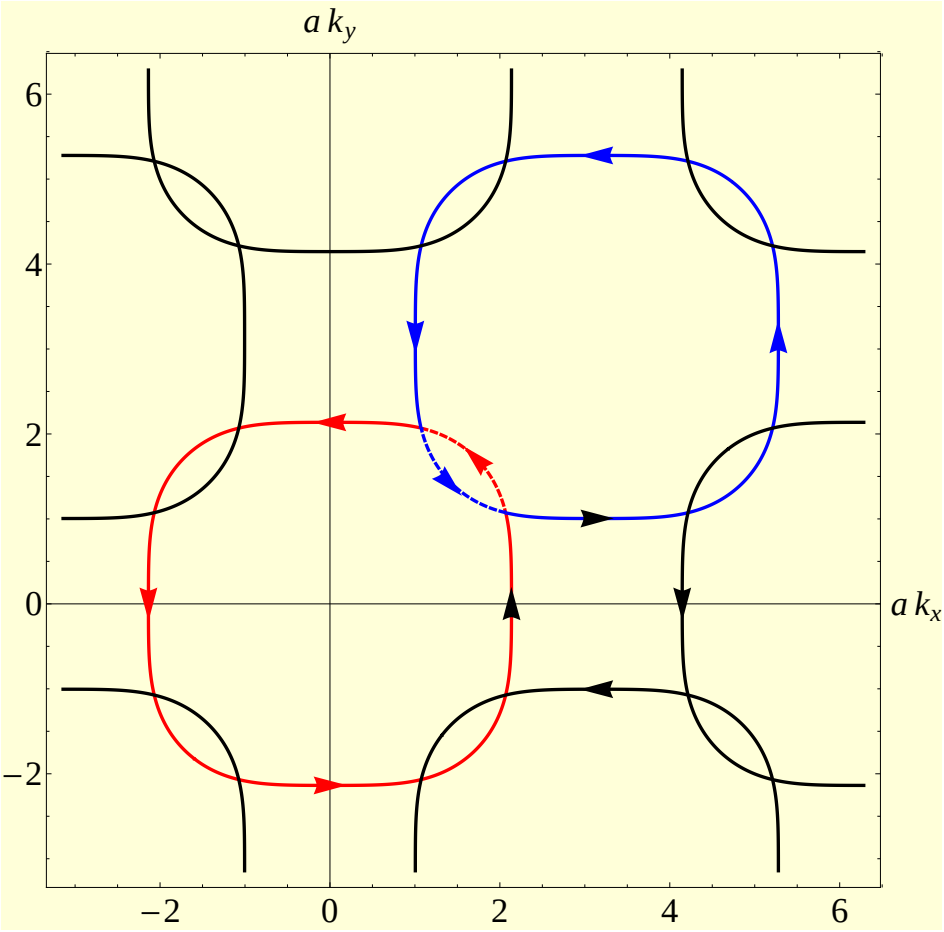

Figure 1.4: Fermi surface in the extended Brillouin zone of NCCO with $x = 0.17$ doping. This plot shows the breakdown junctions and electron trajectories across those junctions. Curves with black arrows represent electron pocket, red and blue dashed lines together form hole pocket, and red solid and dashed curves are corresponding to the very high frequency measured in the experiment.

pockets are most vulnerable to any disorder and unseen in the numerical calculation of S-dH oscillations.

In the calculation of magnetic breakdown effect, more acurate band structure in the equation 1.7 is used. In the previous calculation, only nearest neighbor hopping and the next nearest neighbor hopping terms are considered; for present problem the third neighbor hoppings are added. Downside is more load of numerical calculation; When the third nearest neighbor of band structure is in effect, the transmission matrix combines five consecutive slices(Ψ_{n-2}, Ψ_{n-1},..., and Ψ_{n+2}) instead of three. Thus, the size of the transmission matrices becomes $4M \times 4M$ instead of $2M \times 2M$. And the equation 1.12 is extended to:

$$\begin{bmatrix} \Psi_{n+2} \\ \Psi_{n+1} \\ \Psi_n \\ \Psi_{n-1} \end{bmatrix} = \begin{bmatrix} T_n^{-1}A_n & T_n^{-1}B_n & T_n^{-1}C_n & T_n^{-1}D_n \\ 1 & 0 & 0 & 0 \\ 0 & 1 & 0 & 0 \\ 0 & 0 & 1 & 0 \end{bmatrix} \begin{bmatrix} \Psi_{n+1} \\ \Psi_n \\ \Psi_{n-1} \\ \Psi_{n-2} \end{bmatrix} = \mathbf{T}_n \begin{bmatrix} \Psi_{n+1} \\ \Psi_n \\ \Psi_{n-1} \\ \Psi_{n-2} \end{bmatrix} \tag{1.17}$$

where T_n, A_n, B_n, C_n, D_n are $M \times M$ matrices and the details are given in the chapter 3. The larger size of matrices slows down the calculation but it is worth introducing the third neighbor hopping term in that it can depict electron system more precisely.

1.5 Hole-doped

In chapter 4, quantum oscillation in the hole-doped superconductor $YBa_2Cu_3O_{6+\delta}$ (YBCO) is thoroughly studied. The quantum oscillations in the Hall coefficient (R_H) of YBCO in high magnetic field between 35-62T was observed [13] and frequency around 600T is measured in Shubnikov-de Haas (S-dH) oscillations. [14, 15] It is corresponding to the electron pockets of reconducturcted Fermi surface due to a density wave order. Therefore, it is important to figure out what type of particle-hole pairing order induces Fermi surface reconstruction. At first, a two-fold commensurate d-density wave order was suggested to resolve this YBCO problem. But the absence of hole-poket frequency in quantum oscillations cannot be explained well. [16] Therefore, period-8 d-density wave (dDW) order with spin singlet is

introduced. According to Landau theory, a period-8 dDW order induces a period-4 charge density wave (CDW) order, which is consistent with the nuclear magnetic resonance (NMR) measurement. [17]

The amplitudes of dDW and CDW order parameter are tuned in order to capture features as follows. Electron pockets from reconstructed Fermi surface should be more dominant than hole pockets in order to explain the negative Hall coefficient of YBCO sample. At first glance, the dominance of electron pockets seems contradict to the fact that YBCO is a hole-doped superconductor. But total area spanned by all the small hole pockets is larger than area of electron pockets even though an individual hole pocket is smaller than an electron pocket(see figure 1.5). Slow oscillation frequency arising from small hole pockets is not observed because experiments can catch no more than just a few periods of this slow oscillation. Surely, S-dH measurement in much higher fields may reveal an evidence of hole-pocket frequency ($250T$). Recent measurement up to $85T$ shows a partial evidence but further experiments are required for its confirmation. [18]

There is controversy over whether the field range of experiment above totally suppress superconductivity or not. However, even if superconductivity is only *partially* destroyed and vortices exist in the samples, these vortices can be treated as merely disorder. Along with a period-8 d-wave particle-hole pairing order, this period-4 charge modulation forms 8×8 Hamiltonian in reduced Brillouin zone. Then, Hamiltonian in the coordinate space contains both period-4 site charge modulation and period-8 bond current modulation. Charge modulation is incorporated with $\epsilon_{\mathbf{r}}$ in equation 1.9: $2V_c cos(\frac{\pi r_x}{2a})$ where V_c is the intensity of charge modulation. Period-8 d-density wave order is more complicated in coordinate space and equation 1.10 becomes

$$\frac{iW_0}{2}(-1)^{m'+n'}\ \tilde{U}_{\mathbf{r}',\mathbf{r}}, \tag{1.18}$$

where $m'a = r'_x$ and $n'a = r'_y$. And $\tilde{U}_{\mathbf{r}',\mathbf{r}}$ is as below:

$$\begin{aligned}\tilde{U}_{\mathbf{r}',\mathbf{r}} =& \left[\frac{1+\cos 2\pi\eta}{2}(\delta_{\mathbf{r}',\mathbf{r}+a\hat{\mathbf{x}}} + \delta_{\mathbf{r}',\mathbf{r}-a\hat{\mathbf{x}}}) - (\delta_{\mathbf{r}',\mathbf{r}+a\hat{\mathbf{y}}} + \delta_{\mathbf{r}',\mathbf{r}-a\hat{\mathbf{y}}})\right]\cos 2m'\pi\eta \\ &+ \frac{\sin 2\pi\eta \sin 2m'\pi\eta}{2}(\delta_{\mathbf{r}',\mathbf{r}+a\hat{\mathbf{x}}} - \delta_{\mathbf{r}',\mathbf{r}-a\hat{\mathbf{x}}}),\end{aligned} \tag{1.19}$$

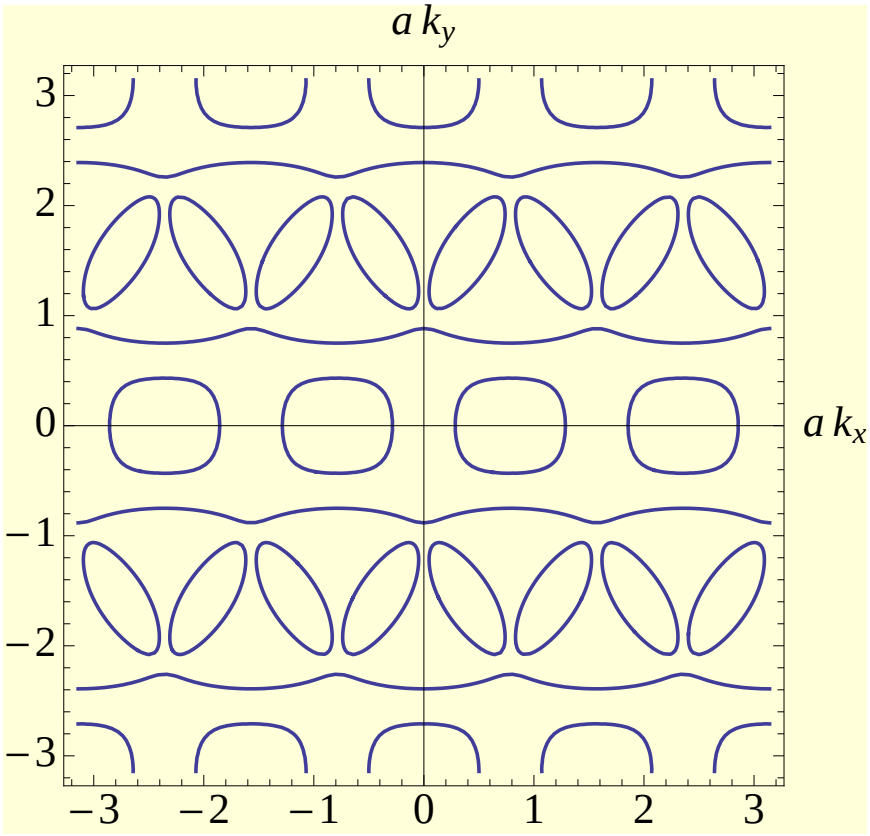

Figure 1.5: Reconstructed Fermi surfaces with period-8 d-density wave order. Details about parameters are given in the chapter 4. There are electron pockets, hole pockets and open orbits. The electron pocket frequency corresponds to 530 T and the hole pockets to 280 T. The doping corresponds to 12.46%. Note that the figure is shown in the extended Brillouin zone for clarity.

where $\eta = \frac{1}{8}$ gives period-8.

In addition, local density of states (LDOS) at Fermi energy is estimated; modulation of LDOS leads to that of Knight shift. Total density of states(DOS) is also derived in order to calculate the specific heat. Detailed calculation is given in the chapter 4. It is also important to choose proper type of disorder: correlation length(l_D) and the intensity of disorder(g_V). This disorder accounts for electric onsite disorders and vortices if superconductivity is not totally suppressed by high magnetic field. In the previous case of NCCO, δ-correlated white noise disorder is used: $l_D = 0$. In contrast, non-zero correlation length is required to obtain clear picture of quantum oscillations in YBCO sample; since YBCO sample is relatively clean compared to NCCO sample. [19] This *cleaner* sample is depicted by correlated disorder, which is derived from the white noise disorder by smoothing over coordinate space as below:

$$V(\mathbf{R}) = \frac{g_V}{2\pi l_D^2} \int d\mathbf{x}\ e^{-\frac{|\mathbf{R}-\mathbf{x}|^2}{2l_D^2}}\ u(\mathbf{x}), \tag{1.20}$$

Here $u(\mathbf{x})$ is white noise disorder that is used for NCCO; $\langle u(\mathbf{x})\rangle = 0$ and $\langle u(\mathbf{x})u(\mathbf{y})\rangle = \delta(\mathbf{x}-\mathbf{y})$. Above smoothing process partially removes *irregularity*, that is, disorder becomes weaker. This smoothing effect can be understood easily in momentum space. Zero correlation length of disorder $l_D = 0$ is corresponding to infinite scattering vector in the Brillouin zone. Then, quasi-particles moving along electron or hole pockets are more likely to transferred to another pockets which is totally disconnected with the original pockets that quasi-particles resided in. In contrast, non-zero correlation length of disorder is corresponding to finite scattering vector in momentum space, therefore, quasi-particles are less likely to be scattered around. This is how non-zero correlation length of disorder can describe relatively clean cuprate superconductor sample.

Quantum oscillations in electron-doped high-temperature superconductors

Jonghyoun Eun, Xun Jia, and Sudip Chakravarty
Department of Physics and Astronomy, University of California–Los Angeles, Los Angeles, California 90095-1547, USA
(Received 25 August 2010; published 23 September 2010)

Quantum oscillations in hole-doped high-temperature superconductors are difficult to understand within the prevailing views. An emerging idea is that of a putative normal ground state, which appears to be a Fermi liquid with a reconstructed Fermi surface. The oscillations are due to formation of Landau levels. Recently the same oscillations were found in the electron-doped cuprate, $Nd_{2-x}Ce_xCuO_4$, in the optimal to overdoped regime. Although these electron-doped nonstoichiometric materials are naturally more disordered, they strikingly complement the hole-doped cuprates. Here we provide an explanation of these observations from the perspective of density waves using a powerful transfer matrix method to compute the conductance as a function of the magnetic field.

DOI: 10.1103/PhysRevB.82.094515 PACS number(s): 74.72.Ek, 74.20.−z, 74.25.Ha, 74.25.Jb

I. INTRODUCTION

Periodically a class of experiments tend to disturb the status quo of the prevailing views in the area of high-temperature cuprate superconductors. Recent quantum oscillation (QO) experiments[1–8] fall into this category.[9] The first set of experiments were carried out in underdoped high-quality crystals of well-ordered $YBa_2Cu_3O_{6+\delta}$ (YBCO), stoichiometric $YBa_2Cu_4O_8$, and the overdoped single-layer $Tl_2Ba_2CuO_{6+\delta}$.[10]

More recently oscillations are also observed in electron-doped $Nd_{2-x}Ce_xCuO_4$ (NCCO).[11] The measurements in NCCO for 15%, 16%, and 17% doping[11] are spectacular. The salient features are: (1) the experiments are performed in the range 30–64 T, far above the upper critical field, which is about 10 T or less; (2) the material involves single CuO plane, and therefore complications involving chains, bilayers, Ortho-II potential,[12] etc., are absent; (3) stripes[13] may not be germane in this case.[14] It is true, however, that neither spin-density wave (SDW) nor *d*-density wave (DDW) (Ref. 15) are yet directly observed in NCCO in the relevant doping range but QOs seem to require their existence, at least the *field-induced* variety (see, however Ref. 16); (4) these experiments are a tour de force because the sample is nonstoichiometric with naturally greater intrinsic disorder. The effect is therefore no longer confined to a limited class of high-quality single crystals; (5) the authors have also succeeded in seeing the transition from low- to high-frequency oscillations[17] in NCCO as a function of doping.

Here we focus on NCCO. We shall see that disorder plays an important role. Without it is impossible to understand why the slow oscillations damp out below 30 T for 15% and 16% doping, and below 60 T for 17% doping, even though the field range is very high. For 17% doping, where a large hole pocket is observed corresponding to very fast oscillations (inconsistent with any kind of density wave order), the necessity of such high fields can have only one explanation, namely, to achieve a sufficiently large $\omega_c\tau$, where $\omega_c = eB/m^*c$, τ is the scattering lifetime of the putative normal phase, m^* the effective mass, and B the magnetic field. Qualitatively, the Dingle factor, D, that suppresses quantum oscillations is $D=e^{-p\pi/\omega_c\tau}$, where p is the index for the harmonic. Assuming a Fermi velocity, suitably averaged over an orbit to be v_F, the mean-free path $l=v_F\tau$. Thus D can be rewritten as $D=e^{-p\pi\hbar ck_F/eBl}$. A crude measure for k_F is given by expressing the area of an extremal orbit, A, as $A=\pi k_F^2$. By setting $m^*v_F=\hbar k_F$, the explicit dependence on the parameters m^* and v_F was eliminated. Assuming that the mean-free paths for the hole and the electron pockets are more or less the same, not an unreasonable assumption, the larger pockets, with larger k_F, will be strongly suppressed for the same value of the magnetic field because of the exponential sensitivity of D to the pocket size. This argument is consistent with our exact transfer matrix calculation using the Landauer formula for the conductance presented below.

Here we show that the oscillation experiments in NCCO reflect a broken translational symmetry[18] that reconstructs the Fermi surface in terms of electron and hole pockets.[9] The emphasis is not the transfer matrix method itself but its use in explaining a major experiment in some detail. We study both SDW and singlet DDW orders with the corresponding mean-field Hamiltonians. A more refined calculation, beyond the scope of the present paper, will be necessary to see the subtle distinction between the two order parameters.

In Sec. II, we introduce our mean-field Hamiltonians and in Sec. III, we discuss the transfer matrix method for the computation of quantum oscillations of the conductance. Section IV contains the results of our numerical computations and Sec. V our conclusions.

II. MEAN-FIELD HAMILTONIAN

We suggest that the experiments in NCCO can be understood from a suitable normal state because the applied magnetic fields between 30 and 65 T are so far above the upper critical field, which is less than 10 T, that vortex physics and the superconducting gap are not important. Our assumption is that a broken translational symmetry state with an ordering vector $\mathbf{Q}=(\pi/a,\pi/a)$ (a being the lattice spacing) can reconstruct the Fermi surface resulting in two hole pockets and one electron pocket within the reduced Brillouin zone, bounded by the constraints on the wave vectors $k_x \pm k_y = \pm \pi/a$. One challenge here is to understand why the large electron pockets corresponding to 15% and 16% doping re-

TABLE I. The band parameters, the chemical potential, and the mean-field parameters for DDW and SDW used in our calculation. F in tesla corresponds to the calculated oscillation frequencies of the hole pocket, the so-called slow frequencies. The measured F for 15% doping is 290 ± 10 T and for 16% doping is 280 ± 15 T. The calculated magnitude of F does depend on the neglected t''.

Order	t (eV)	t'	W_0	V_S	μ	V_0	F (T)
DDW 15%	0.3	$0.45t$	$0.1t$	*	$-0.40t$	$0.8t$	195
DDW 16%	0.3	$0.45t$	$0.1t$	*	$-0.365t$	$0.8t$	165
SDW 15%	0.3	$0.45t$	*	$0.05t$	$-0.403t$	$0.8t$	195
SDW 16%	0.3	$0.45t$	*	$0.05t$	$-0.366t$	$0.8t$	173

sulting from the band-structure parameters for NCCO defined below are not observed but the much smaller hole pockets are. Another challenge is to understand why the large Fermi surface at 17% doping is not observed until the applied field reaches about 60 T. The reason we believe is the existence strong cation disorder in this material. It is therefore essential to incorporate disorder in our Hamiltonian. For the Hamiltonian itself, we consider a mean-field approach, and for this purpose we consider two possible symmetries, one that corresponds to a singlet in the spin space (DDW) and one that is a triplet in the spin space (SDW). Note that these are particle-hole condensates for which orbital function does not constrain the spin wave function unlike a particle-particle condensate (superconductor) because there are no exchange requirements between a particle and a hole.

We believe that it is reasonable that as long as a system is deep inside a broken symmetry state, mean-field theory and its associated elementary excitations should correctly capture the physics. The fluctuation effects will be important close to quantum phase transitions. However, there are no indications in the present experiments that fluctuations are important. The microscopic basis for singlet DDW Hamiltonian is discussed in some detail in Refs. 19 and 20, and in references therein. So, we do not see any particular need to duplicate this discussion here. The mean-field Hamiltonian for the singlet DDW in real space, in terms of the site-based fermion annihilation and creation operators of spin σ, $c_{\mathbf{i},\sigma}$, and $c^{\dagger}_{\mathbf{i},\sigma}$, is

$$H_{\mathrm{DDW}} = \sum_{\mathbf{i},\sigma} \epsilon_{\mathbf{i}} c^{\dagger}_{\mathbf{i},\sigma} c_{\mathbf{i},\sigma} + \sum_{\mathbf{i},\mathbf{j},\sigma} t_{\mathbf{i},\mathbf{j}} e^{ia_{\mathbf{i},\mathbf{j}}} c^{\dagger}_{\mathbf{i},\sigma} c_{\mathbf{j},\sigma} + \mathrm{H.c.}, \quad (1)$$

where the nearest-neighbor hopping matrix elements are

$$t_{\mathbf{i},\mathbf{i}+\hat{\mathbf{x}}} = -t + \frac{iW_0}{4}(-1)^{(\mathbf{i}_\mathbf{x}+\mathbf{i}_\mathbf{y})}, \quad (2)$$

$$t_{\mathbf{i},\mathbf{i}+\hat{\mathbf{y}}} = -t - \frac{iW_0}{4}(-1)^{(\mathbf{i}_\mathbf{x}+\mathbf{i}_\mathbf{y})}. \quad (3)$$

Here W_0 is the DDW gap. We also include the next-nearest-neighbor hopping t' whereas the third-neighbor hopping t'' is ignored to simplify computational complexity without losing the essential aspects of the problem. The parameters t and t' are chosen (see Table I) to closely approximate the more conventional band structure, as shown in Fig. 1. We have checked that the choice $t''=0$ provides reasonably consistent results for the frequencies in the absence of disorder. For example, for DDW, and 15% doping, the hole pocket frequency is 185 T, and the corresponding electron pocket frequency is 2394 T.

Similarly, the SDW mean-field Hamiltonian is

$$H_{\mathrm{SDW}} = \sum_{\mathbf{i},\sigma} [\epsilon_{\mathbf{i}} + \sigma V_S (-1)^{\mathbf{i}_\mathbf{x}+\mathbf{i}_\mathbf{y}}] c^{\dagger}_{\mathbf{i},\sigma} c_{\mathbf{i},\sigma} + \sum_{\mathbf{i},\mathbf{j},\sigma} t_{\mathbf{i},\mathbf{j}} e^{ia_{\mathbf{i},\mathbf{j}}} c^{\dagger}_{\mathbf{i},\sigma} c_{\mathbf{j},\sigma} + \mathrm{H.c.} \quad (4)$$

and the spin $\sigma = \pm 1$ while the magnitude of the SDW amplitude is V_S. In both cases, a constant perpendicular magnetic field B is included via the Peierls phase factor $a_{\mathbf{i},\mathbf{j}} = \frac{2\pi e}{h} \int_{\mathbf{j}}^{\mathbf{i}} \mathbf{A} \cdot d\mathbf{l}$, where $\mathbf{A} = (0, -Bx, 0)$ is the vector potential in the Landau gauge. We note that usually a perpendicular magnetic field, even as large as 60 T, has little effect on the DDW gap,[21] except close to the doping at which it collapses, where field-induced order may be important.

We have seen previously[19] that the effect of long-ranged correlated disorder is qualitatively similar to white noise insofar as the QOs are concerned. The effect of the nature of

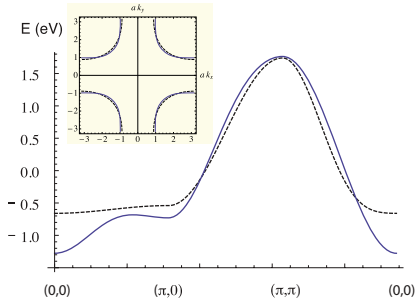

FIG. 1. (Color online) The solid curve represents the t-t'-t'' band structure (t=0.38 eV, $t'=0.32t$, $t''=0.5t'$), and the dashed curve corresponds to t-t' band structure, (see Table I). The quasiparticle energy is plotted in the Brillouin zone along the triangle $(0,0) \rightarrow (\pi,0) \rightarrow (\pi,\pi) \rightarrow (0,0)$. In the inset, the chemical potential, μ, was adjusted to obtain approximately 15% doping.

disorder on the spectral function of angle-resolved photoemission spectroscopy (ARPES) was found to be far more important. The reason is that the coherence factors of the ARPES spectral function are sensitive to the nature of the disorder because they play a role similar to Wannier functions. In contrast, the QOs are damped by the Dingle factor, which is parametrized by a single lifetime and disorder enters in an averaged sense.

Thus, it is sufficient to consider on-site disorder. The on-site energy is δ-correlated white noise defined by the disorder average $\overline{\epsilon_i}=0$ and $\overline{\epsilon_i \epsilon_j}=V_0^2\delta_{i,j}$. For an explicit calculation, we need to choose the band-structure parameters, W_0, V_S, and the disorder magnitude V_0. When considering the magnitude of disorder one should keep in mind that the full bandwidth is $8t$. The magnetic field ranges roughly between 30 and 64 T, representative of the experiments in NCCO. The magnetic length is $l_B=\sqrt{\hbar/eB}$, which for $B=30$ T is approximately $12a$, where the lattice constant a is equal to 3.95 Å.

The effect of potential scattering that modulates charge density is indirect on twofold commensurate SDW or DDW order parameter,[22] mainly because SDW is modulation of spin and DDW that of charge current. Thus, the robustness of these order parameters with respect to disorder protects the corresponding quasiparticle excitations insofar as quantum oscillations are concerned, as seen below in our exact numerical calculations. Thus we did not find it important to study this problem self consistently.

III. TRANSFER MATRIX METHOD

The transfer matrix method and the calculation of the Lyapunov exponents sketched elsewhere[19] is fully described here for the case of singlet DDW; for SDW the generalization is straightforward, where the diagonal term must be modified because of V_S, and the term W_0 will be absent. Consider a quasi-one-dimensional system, $L \gg M$, with a periodic boundary condition along y direction. Let $\Psi_n=(\psi_{n,1},\psi_{n,2},\ldots,\psi_{n,M})^T$ be the amplitudes on the slice n for an eigenstate with a given energy, then the amplitudes on three successive slices satisfy the relation

$$\begin{bmatrix} \Psi_{n+1} \\ \Psi_n \end{bmatrix} = \begin{bmatrix} T_n^{-1}A_n & -T_n^{-1}B_n \\ 1 & 0 \end{bmatrix} \begin{bmatrix} \Psi_n \\ \Psi_{n-1} \end{bmatrix} = \mathbf{T}_n \begin{bmatrix} \Psi_n \\ \Psi_{n-1} \end{bmatrix}, \tag{5}$$

where T_n, A_n, and B_n are $M \times M$ matrices. The nonzero matrix elements of the matrix A_n are

$$(A_n)_{m,m} = \epsilon_{n,m} - \mu,$$

$$(A_n)_{m,m+1} = \left[-t + \frac{iW_0}{4}(-1)^{m+n} \right] e^{-in\phi},$$

$$(A_n)_{m,m-1} = \left[-t + \frac{iW_0}{4}(-1)^{m+n} \right] e^{in\phi}, \tag{6}$$

where $\phi=2\pi Ba^2e/h$ is a constant. For the matrix B_n,

$$(B_n)_{m,m} = -\left[-t - \frac{iW_0}{4}(-1)^{m+n} \right],$$

$$(B_n)_{m,m+1} = -t' e^{i(-n+1/2)\phi},$$

$$(B_n)_{m,m-1} = -t' e^{i(n-1/2)\phi}. \tag{7}$$

For the matrix T_n, we note that $T_n=B_{n+1}^{\dagger}$.

The $2M$ Lyapunov exponents, γ_i, of $\lim_{N\to\infty}(\mathcal{T}_N\mathcal{T}_N^{\dagger})^{1/2N}$, where $\mathcal{T}_N=\Pi_{j=1}^{j=N}\mathbf{T}_j$, are defined by the corresponding eigenvalues $\lambda_i=e^{\gamma_i}$. All Lyapunov exponents $\gamma_1>\gamma_2>\ldots>\gamma_{2M}$, are computed by a procedure given in Ref. 23. The modification here is that this matrix is not symplectic. Therefore all $2M$ eigenvalues have to be computed. The remarkable fact, however, is that except for a small fraction, consisting of larger eigenvalues, the rest do come in pairs $(\lambda, 1/\lambda)$, as for the symplectic case, within numerical accuracy. We have no analytical proof of this curious fact. Clearly, larger eigenvalues contribute insignificantly to the more general formula for the conductance,[24]

$$\sigma(B) = \frac{e^2}{h}\mathrm{Tr}\sum_{j=1}^{2M} \frac{2}{(\mathcal{T}_N\mathcal{T}_N^{\dagger}) + (\mathcal{T}_N\mathcal{T}_N^{\dagger})^{-1} + 2}. \tag{8}$$

When the eigenvalues do come in pairs, the conductance formula simplifies to the more common Landauer formula,[25]

$$\sigma_{xx}(B) = \frac{e^2}{h}\sum_{i=1}^{M} \frac{1}{\cosh^2(M\gamma_i)}. \tag{9}$$

The transfer matrix method is a very powerful method and the results obtained are rigorous compared to *ad hoc* broadening of the Landau levels, which also require more adjustable parameters to explain the experiments. Once the distribution of disorder is specified there are no further approximations. We note that the values of M were chosen to be much larger than our previous work,[19] at least 128 (that is, 128 a in physical units) and sometimes as large as 512. The length of the strip L is varied between 10^5 and 10^6. This easily led to an accuracy better than 5% for the smallest Lyapunov exponent, γ_i, in all cases.

We have calculated the ab-plane conductance but the measured c-axis resistance, R_c, is precisely related to it, at least as far as the oscillatory part is concerned. This can be seen from the arguments in Ref. 26. Although the details can be improved, the crux of the argument is that the planar density of states enters R_c: the quasiparticle scatters many times in the plane while performing cyclotron motion before hopping from plane to plane (measured ab-plane resistivity is of the order 10 $\mu\Omega$ cm as compared to 1 Ω cm for the c-axis resistivity even at optimum doping[14]). It is worth noting that oscillations of R_c also precisely follows the oscillations of the magnetization in overdoped $Tl_2Ba_2CuO_{6+\delta}$.[10]

IV. RESULTS

There are clues in the experiments[11] that disorder is very important. For 15% and 16% doping, the slow oscillations in experiments, of frequency 290–280 T, are not observed until the field reaches above 30 T, which is much greater than $H_{c2}<10$ T. For 17% doping the onset of fast oscillations at a frequency of 10,700 T are strikingly not observable until

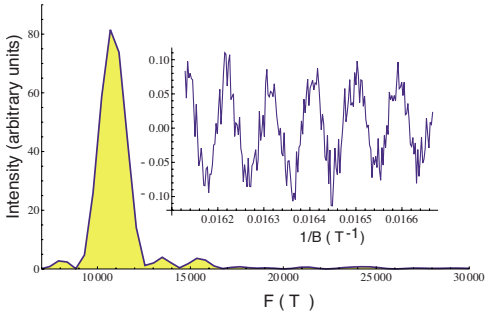

FIG. 2. (Color online) The main plot shows the Fourier transform of the field sweep shown in the inset. The peak is at 10 695 T. The inset is a smooth background subtracted Shubnikov de Haas oscillations, as calculated from the Landauer formula for 17% doping as a function of $1/B$. The disorder parameter is $V_0=0.7t$. The band-structure parameters are given in Table I.

the field reaches 60 T. The estimated scattering time from the Dingle factor at even optimal doping and at 4 K is quite short.

For 17% doping corresponding to $\mu=-0.322t$ and the band structure given in Table I, a slight change in disorder from $V_0=0.7t$ to $V_0=0.8t$ makes the difference between a clear observation of a peak to simply noise within the field sweep between 60 and 62 T, as shown in Figs. 2 and 3. Since in this case $W_0=V_S=0$, there is little else to blame for the disappearance of the oscillations for fields roughly below 60 T. The results are essentially identical for small values of W_0, such as $0.025t$.

For 15% and 16% dopings, we chose V_0 to simulate the fact that oscillations seem to disappear below 30 T. The field sweep was between 30 and 60 T. The results for DDW order are shown in Figs. 4 and 5.

The most remarkable feature of these figures is that disorder has completely wiped out the large electron pocket leaving the small hole pocket visible. To emphasize this

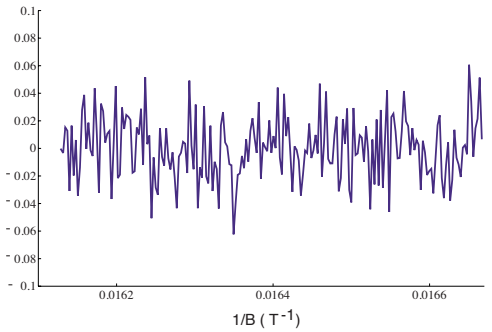

FIG. 3. (Color online) The same parameters as in Fig. 2 but $V_0=0.8t$. The background subtracted conductance is simply noise to an excellent approximation.

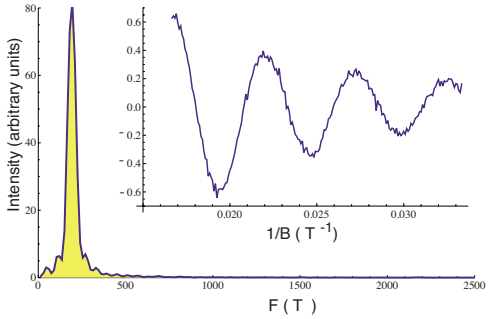

FIG. 4. (Color online) The same plot as in Fig. 2, except for 15% doping and DDW order. The parameters are given in Table I.

point, we also plot the results for 15% doping but with much smaller disorder $V_0=0.2t$; see Fig. 6. Now we can see the fragmented remnants of the electron pocket. With further lowering of disorder, the full electron pocket becomes visible. It is clear that disorder has a significantly stronger effect on the electron pockets than on the hole pockets. This, as we noted earlier, is largely due to higher density of states around the antinodal points, which significantly accentuates the effect of disorder.[19]

We have done parallel calculations with SDW order as well. The results are essentially identical. They are shown again for 15% and 16% doping in Figs. 7 and 8. We have kept all parameters fixed while adjusting the SDW gap to achieve as best an approximation to experiments as possible.

It is important to summarize our results in the context of experimental observations. First, we were able to show that the electron pocket frequencies are strikingly absent because of disorder and the slow frequencies corresponding to the hole pocket for 15% and 16% doping damp out below about 30 T, even though H_{c2} is less than 10 T. Similarly, that the high-frequency oscillations at 17% doping do not arise until about 60 T has a natural explanation in terms of disorder, although in this case some magnetic breakdown effect, which was not explored, can be expected. This requires both

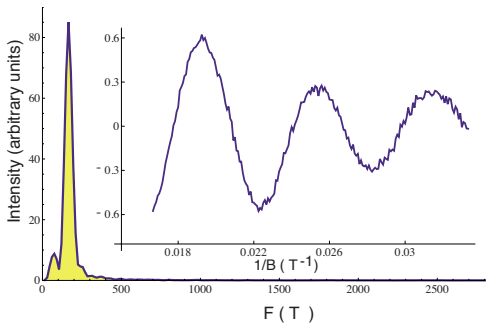

FIG. 5. (Color online) The same plot as in Fig. 2, except for 16% doping and DDW order. The parameters are given in Table I.

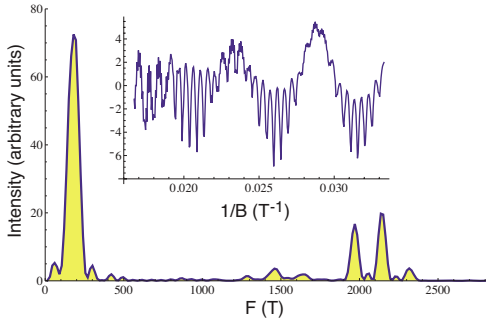

FIG. 6. (Color online) The same plot as in Fig. 4, except that V_0=0.2t instead of 0.8t. There is now a fragmented electron pocket centered around 2100 T and the main peak is at 183 T. The rest of the parameters are given in Table I.

further experimental and theoretical investigations. The calculated frequency of the high-frequency oscillations, 10 695 T is remarkably close to experimental value of 10, 700 ± 400 T. As to the magnitude of the slow oscillations, the calculated values are given in Table I, which are reasonable in both magnitude and trend when compared to experiments. The small discrepancies in the magnitude of F are due to our neglect of t'' in the band structure. This can be, and was, checked by checking the pure case, that is, without disorder.

V. CONCLUSIONS

In the absence of disorder or thermal broadening, the oscillation waveforms are never sinusoidal in two dimensions and contain many Fourier harmonics. At zero temperature, moderate disorder converts the oscillations to sinusoidal waveform with rapidly decreasing amplitudes of the harmonics. Further increase in disorder ultimately destroys the amplitudes altogether. Many experiments exhibit roughly sinusoidal waveform at even ultralow temperatures, implying

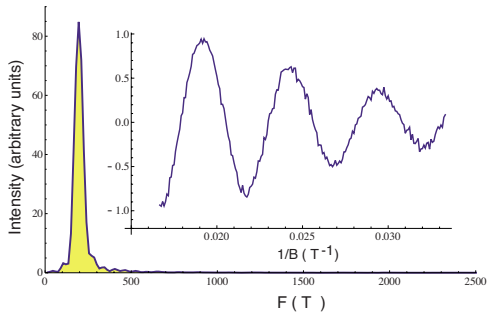

FIG. 7. (Color online) The same plot as in Fig. 4 for 15% doping but using SDW order. The main peak is at 195 T. The rest of the parameters are given in Table I.

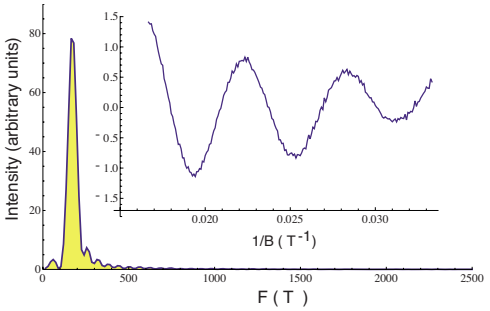

FIG. 8. (Color online) The same plot as in Fig. 7, except for 16% doping and using SDW order. The main peak is at 173 T. The rest of the parameters are given in Table I.

that disorder is important. The remarkably small electronic dispersion in the direction perpendicular to the CuO planes cannot alone account for the waveform.

For NCCO it is no longer a mystery as to why the frequency corresponding to the larger electron pocket is not observed. As we have shown, disorder is the culprit. Neither is the comparison with ARPES controversial,[14] as in the case of YBCO, since there is good evidence of Fermi-surface crossing in the direction $(\pi,0)\rightarrow(\pi,\pi)$, which is a signature of the electron pocket. The crossing along $(\pi,\pi)\rightarrow(0,0)$ can be easily construed as an evidence of a small hole pocket for which half of it is made invisible both from the coherence factors and disorder effects.[19] For electron-doped materials, such as NCCO and PCCO, it is known[14] that the Hall coefficient changes sign around 17% doping and therefore the picture of reconnection of the Fermi pockets is entirely plausible, with some likely magnetic breakdown effects. The real question is what is the evidence of SDW or DDW in the relevant doping range between 15% and 17%. From neutron measurements, we know that there is no long-range SDW order for doping above 13.4%.[27] We cannot rule out field-induced SDW at about 30 T. For DDW, there are no corresponding neutron measurements to observe its existence. Given that DDW is considerably more hidden[15,28] from common experiments, it is more challenging to establish it directly. NMR experiments in high fields for suitable nuclei can shed light on this question. The unavoidable logical conclusion from the QO measurements is that a density wave that breaks translational symmetry must be present. We suggest that motivated future experiments will be necessary to reach a definitive conclusion. Finally, at the level of mean-field theory we have been unable to decide between SDW and singlet DDW. At the moment the best recourse is to experimentally look for spin zeros in the amplitude of quantum oscillations in a tilted magnetic field. A theoretical discussion of this phenomenon that can potentially shed light between a triplet order parameter (SDW) and a singlet order parameter, the singlet DDW discussed here, was provided recently.[29] So far experiments are in conflict with each other in YBCO: one group suggests a triplet order parameter[30,31] and the other a singlet order parameter.[32]

It is unquestionable that the QO experiments are likely to change the widespread views in the field of high-temperature

superconductivity. Although the measurements in YBCO are not fully explained, the measurements in NCCO appear to have a clear and simple explanation, as shown here. However, given the similarity of the phenomenon in both hole- and electron-doped cuprates, it is likely that the quantum oscillations have the same origin.

ACKNOWLEDGMENTS

This work is supported by NSF under the Grant No. DMR-0705092. All calculations were performed at Hoffman 2 Cluster at UCLA. We thank E. Abrahams for a critical reading of the manuscript and N. P. Armitage for comments.

[1] N. Doiron-Leyraud, C. Proust, D. LeBoeuf, J. Levallois, J.-B. Bonnemaison, R. Liang, D. A. Bonn, W. N. Hardy, and L. Taillefer, Nature (London) **447**, 565 (2007).
[2] A. F. Bangura *et al.*, Phys. Rev. Lett. **100**, 047004 (2008).
[3] D. LeBoeuf *et al.*, Nature (London) **450**, 533 (2007).
[4] C. Jaudet *et al.*, Phys. Rev. Lett. **100**, 187005 (2008).
[5] E. A. Yelland, J. Singleton, C. H. Mielke, N. Harrison, F. F. Balakirev, B. Dabrowski, and J. R. Cooper, Phys. Rev. Lett. **100**, 047003 (2008).
[6] S. E. Sebastian, N. Harrison, E. Palm, T. P. Murphy, C. H. Mielke, R. Liang, D. A. Bonn, W. N. Hardy, and G. G. Lonzarich, Nature (London) **454**, 200 (2008).
[7] A. Audouard, C. Jaudet, D. Vignolles, R. Liang, D. A. Bonn, W. N. Hardy, L. Taillefer, and C. Proust, Phys. Rev. Lett. **103**, 157003 (2009).
[8] J. Singleton *et al.*, Phys. Rev. Lett. **104**, 086403 (2010).
[9] S. Chakravarty, Science **319**, 735 (2008).
[10] B. Vignolle, A. Carrington, R. A. Cooper, M. M. J. French, A. P. Mackenzie, C. Jaudet, D. Vignolles, C. Proust, and N. E. Hussey, Nature (London) **455**, 952 (2008).
[11] T. Helm, M. V. Kartsovnik, M. Bartkowiak, N. Bittner, M. Lambacher, A. Erb, J. Wosnitza, and R. Gross, Phys. Rev. Lett. **103**, 157002 (2009).
[12] D. Podolsky and H.-Y. Kee, Phys. Rev. B **78**, 224516 (2008).
[13] A. J. Millis and M. R. Norman, Phys. Rev. B **76**, 220503 (2007).
[14] N. Armitage, P. Fournier, and R. Green, Rev. Mod. Phys. **82**, 2421 (2010).
[15] S. Chakravarty, R. B. Laughlin, D. K. Morr, and C. Nayak, Phys. Rev. B **63**, 094503 (2001).
[16] P. Rourke, A. Bangura, C. Proust, J. Levallois, N. Doiron-Leyraud, D. LeBoeuf, L. Taillefer, S. Adachi, M. Sutherland, and N. Hussey, Phys. Rev. B **82**, 020514(R) (2010).
[17] C. Kusko, R. S. Markiewicz, M. Lindroos, and A. Bansil, Phys. Rev. B **66**, 140513 (2002).
[18] S. Chakravarty and H.-Y. Kee, Proc. Natl. Acad. Sci. U.S.A. **105**, 8835 (2008).
[19] X. Jia, P. Goswami, and S. Chakravarty, Phys. Rev. B **80**, 134503 (2009).
[20] I. Dimov, P. Goswami, X. Jia, and S. Chakravarty, Phys. Rev. B **78**, 134529 (2008).
[21] H. K. Nguyen and S. Chakravarty, Phys. Rev. B **65**, 180519 (2002).
[22] A. Ghosal and H.-Y. Kee, Phys. Rev. B **69**, 224513 (2004).
[23] B. Kramer and M. Schreiber, in *Computational Physics*, edited by K. H. Hoffmann and M. Schreiber (Springer, Berlin, 1996), p. 166.
[24] J. L. Pichard and G. André, Europhys. Lett. **2**, 477 (1986).
[25] D. S. Fisher and P. A. Lee, Phys. Rev. B **23**, 6851 (1981).
[26] N. Kumar and A. M. Jayannavar, Phys. Rev. B **45**, 5001 (1992).
[27] E. M. Motoyama, G. Yu, I. M. Vishik, O. P. Vajk, P. K. Mang, and M. Greven, Nature (London) **445**, 186 (2007).
[28] C. Nayak, Phys. Rev. B **62**, 4880 (2000).
[29] D. Garcia-Aldea and S. Chakravarty, arXiv:1008.2030 (unpublished).
[30] S. E. Sebastian, N. Harrison, C. H. Mielke, R. Liang, D. A. Bonn, W. N. Hardy, and G. G. Lonzarich, Phys. Rev. Lett. **103**, 256405 (2009).
[31] S. E. Sebastian, N. Harrison, P. A. Goddard, M. M. Altarawneh, C. H. Mielke, R. Liang, D. A. Bonn, W. N. Hardy, O. K. Andersen, and G. G. Lonzarich, Phys. Rev. B **81**, 214524 (2010).
[32] B. Ramshaw, B. Vignolle, J. Day, R. Liang, W. Hardy, C. Proust, and D. Bonn, arXiv:1004.0260 (unpublished).

Magnetic breakdown and quantum oscillations in electron-doped high-temperature superconductor $Nd_{2-x}Ce_xCuO_4$

Jonghyoun Eun and Sudip Chakravarty
Department of Physics and Astronomy, University of California Los Angeles, Los Angeles, California 90095-1547, USA
(Received 8 July 2011; published 12 September 2011)

Recent, more precise experiments have revealed both a slow and a fast quantum oscillation in the c-axis resistivity of nearly optimal to overdoped electron-doped high-temperature superconductor $Nd_{2-x}Ce_xCuO_4$. Here, we study this problem from the perspective of Fermi surface reconstruction using an exact transfer matrix method and the Pichard-Landauer formula. In this method, neither quasiclassical approximations for magnetic breakdown nor *ad hoc* broadening of Landau levels is necessary to study the high-field quantum oscillations. The underlying Hamiltonian is a mean-field Hamiltonian that incorporates a twofold commensurate Fermi surface reconstruction. While the specific mean field considered is the d-density wave, similar results can also be obtained by a model of a spin density wave, as was explicitly demonstrated earlier. The results are consistent with an interplay of magnetic breakdown across small gaps in the reconstructed Fermi surface and Shubnikov–de Haas oscillations.

DOI: 10.1103/PhysRevB.84.094506 PACS number(s): 74.72.Ek, 74.25.Jb, 74.25.Ha, 74.20.−z

I. INTRODUCTION

Quantum oscillations were first discovered[1] in the Hall coefficient of a hole-doped high-temperature superconductor $YBa_2Cu_3O_{6+\delta}$ (YBCO) at high magnetic fields between 35 and 62 T in the underdoped regime close to 10%. Since then, a number of measurements, in even higher fields and with greater precision using a variety of measurement techniques, have confirmed the basic features of this experiment. However, the precise mechanism responsible for oscillations has become controversial.[2] Fermi surface reconstruction due to a density wave order that could arise if superconductivity is "effectively destroyed" by high magnetic fields has been the focus of some attention.[3]

In contrast, similar quantum oscillation measurements in the doping range 15–17% in $Nd_{2-x}Ce_xCuO_4$ (NCCO)[4] seem easier to interpret, as the magnetic field range 30–65 T is far above the upper critical field, which is less than 10 T. This clearly places the material in the "normal" state, a source of contention in measurements in YBCO; in NCCO, the crystal structure consists of a single CuO plane per unit cell, and, in contrast to YBCO, there are no complicating chains, bilayers, ortho-II potential, stripes, etc.[5] Thus, it would appear to be ideal for gleaning the mechanism of quantum oscillations. On the other hand, disorder in NCCO is significant. It is believed that well-ordered chain materials of YBCO contain much less disorder by comparison.

In a previous publication,[6] we mentioned in passing that it is not possible to understand the full picture in NCCO without magnetic breakdown effects, since the gaps are expected to be very small in the relevant regime of the parameter space. However, in that preliminary work, the breakdown phenomenon was not addressed; instead, we focused our attention on the effect of disorder. Since then, recent measurements[7,8] have indeed revealed magnetic breakdown in the range 16–17% doping, almost to the edge of the superconducting dome. Here, we consider the same transfer matrix method used previously,[6] but we include third-neighbor hopping of electrons on the square planar lattice, without which many experimental aspects cannot be faithfully reproduced, including quantitative estimates of the oscillation frequencies and breakdown effects. The third-neighbor hopping makes the numerical transfer matrix calculation more intensive because of the enlarged size of the matrix, but we were able to overcome the technical challenges. In this paper, we also analyze the c-axis resistivity and the absence of the electron pockets in the experimental regime.

II. HAMILTONIAN

The mean-field Hamiltonian for a d-density wave[9] (DDW) in real space, in terms of the site-based fermion annihilation and creation operators $c_{\mathbf{i}}$ and $c_{\mathbf{i}}^\dagger$, is

$$H_{\mathrm{DDW}} = \sum_{\mathbf{i}} \epsilon_{\mathbf{i}} c_{\mathbf{i}}^\dagger c_{\mathbf{i}} + \sum_{\mathbf{i},\mathbf{j}} t_{\mathbf{i},\mathbf{j}} e^{i a_{\mathbf{i},\mathbf{j}}} c_{\mathbf{i}}^\dagger c_{\mathbf{j}} + \mathrm{H.c.}, \tag{1}$$

where the nearest-neighbor hopping matrix elements include a DDW gap W_0 and are

$$\begin{aligned} t_{\mathbf{i},\mathbf{i}+\hat{\mathbf{x}}} &= -t + \tfrac{iW_0}{4}(-1)^{(n+m)}, \\ t_{\mathbf{i},\mathbf{i}+\hat{\mathbf{y}}} &= -t - \tfrac{iW_0}{4}(-1)^{(n+m)}, \end{aligned} \tag{2}$$

where (n,m) are a pair of integers labeling a site: $\mathbf{i} = n\hat{\mathbf{x}} + m\hat{\mathbf{y}}$; the lattice constant a will be set to unity unless otherwise specified. In this paper, we also include both the next-nearest-neighbor hopping matrix element, t', and the third-nearest-neighbor hopping matrix element, t''. A constant perpendicular magnetic field B is included via the Peierls phase factor $a_{\mathbf{i},\mathbf{j}} = \frac{e}{\hbar c}\int_{\mathbf{j}}^{\mathbf{i}} \mathbf{A}\cdot d\mathbf{l}$, where $\mathbf{A} = (0, -Bx, 0)$ is the vector potential in the Landau gauge. The band parameters are chosen to be $t = 0.38$ eV, $t' = 0.32t$, and $t'' = 0.5t'$.[10] The chemical potential μ is adjusted to achieve the required doping level and is given in Table I, as is the DDW gap W_0. We assume that the on-site energy is δ-correlated white noise defined by the disorder average $\overline{\epsilon_{\mathbf{i}}} = 0$ and $\overline{\epsilon_{\mathbf{i}}\epsilon_{\mathbf{j}}} = V_0^2\delta_{\mathbf{i},\mathbf{j}}$. Disorder levels for each of the cases studied are also given in Table I. The range of parameters chosen covered the estimates made in Ref. 8. We have seen previously that longer-ranged correlated disorder led to very similar results.[11]

TABLE I. Parameters W_0 (DDW gap), V_0 (on-site disorder potential), and μ (chemical potential).

Figure	Gap W_0 (meV)	μ	doping (%)
Fig. 2	5	$0.057t$	17
Fig. 3	10	$0.057t$	17
Fig. 4	15	$0.0176t$	16
Fig. 5	30	$0.0176t$	16

The Fermi surface areas (see Fig. 1) of the small hole pocket in the absence of disorder correspond to oscillation frequencies 330 T at 15% doping, 317 T at 16% doping, and 291 T at 17% doping. These frequencies seem to be insensitive to W_0 within the range given in Table I.

III. THE TRANSFER MATRIX METHOD

The transfer matrix to compute the oscillations of the conductance is a powerful method. It requires neither a quasiclassical approximation to investigate magnetic breakdown nor *ad hoc* broadening of the Landau level to incorporate the effect of disorder. Various models of disorder, both long- and short-ranged, can be studied *ab initio*. The mean-field Hamiltonian, being a quadratic noninteracting Hamiltonian, leads to a Schrödinger equation for the site amplitudes, which is then recast in the form of a transfer matrix; the full derivation is given in the Appendix. The conductance is then calculated by a formula that is well known in the area of mesoscopic physics, namely the Pichard-Landauer formula.[12] This yields Shubnikov–de Haas oscillations of the *ab*-plane resistivity, ρ_{ab}. We show later how this can be related to the *c*-axis resistivity ρ_c measured in experiments.

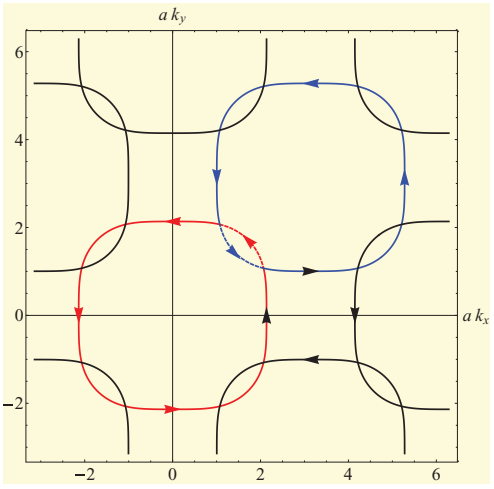

FIG. 1. (Color online) A plot showing the breakdown junctions and electron trajectories across them in the extended Brillouin zone. The figure corresponds to NCCO with 17% doping and a small DDW gap. Note that the reflection at the junctions involves a large change in momentum. The electron trajectories that lead to magnetic breakdown of small hole pockets are shown.

Consider a quasi-1D system, $N \gg M$, with a periodic boundary condition along the y direction. Here, Na is the length in the x direction and Ma is the length in the y direction, a being the lattice spacing. Let $\Psi_n = (\psi_{n,1}, \psi_{n,2}, \ldots, \psi_{n,M})^T$, $n = 1, \ldots, N$, be the amplitudes on the slice n for an eigenstate with a given energy. Then the amplitudes on four successive slices must satisfy the relation

$$\begin{bmatrix} \Psi_{n+2} \\ \Psi_{n+1} \\ \Psi_n \\ \Psi_{n-1} \end{bmatrix} = \begin{bmatrix} U_n^{-1}A_n & U_n^{-1}B_n & U_n^{-1}C_n & U_n^{-1}D_n \\ 1 & 0 & 0 & 0 \\ 0 & 1 & 0 & 0 \\ 0 & 0 & 1 & 0 \end{bmatrix} \begin{bmatrix} \Psi_{n+1} \\ \Psi_n \\ \Psi_{n-1} \\ \Psi_{n-2} \end{bmatrix} = \mathbf{T}_n \begin{bmatrix} \Psi_{n+1} \\ \Psi_n \\ \Psi_{n-1} \\ \Psi_{n-2} \end{bmatrix}, \tag{3}$$

where U_n, A_n, B_n, C_n, and D_n are $M \times M$ matrices. The nonzero matrix elements of matrix A_n are

$$(A_n)_{m,m} = -\left[-1 - \frac{iW_0}{4}(-1)^{m+n}\right], \tag{4}$$

$$(A_n)_{m,m+1} = -t' e^{i(-n-\frac{1}{2})\phi}, \tag{5}$$

$$(A_n)_{m,m-1} = -t' e^{i(n+\frac{1}{2})\phi}, \tag{6}$$

where $\phi = Ba^2e/\hbar c$ is a constant. The elements of the matrix B_n are

$$(B_n)_{m,m} = \epsilon_{n,m} - \mu, \tag{7}$$

$$(B_n)_{m,m+1} = \left[-1 + \frac{iW_0}{4}(-1)^{m+n}\right] e^{-in\phi}, \tag{8}$$

$$(B_n)_{m,m-1} = \left[-1 + \frac{iW_0}{4}(-1)^{m+n}\right] e^{in\phi}, \tag{9}$$

$$(B_n)_{m,m+2} = t'' e^{-i2n\phi}, \tag{10}$$

$$(B_n)_{m,m-2} = t'' e^{i2n\phi}. \tag{11}$$

Here $C_n = A_n^\dagger$ and $D_n = -U_n = t''\mathbb{1}$, where $\mathbb{1}$ is the $M \times M$ identity matrix.

The $4M$ Lyapunov exponents, γ_i, of $\lim_{N\to\infty}(\mathcal{T}_N\mathcal{T}_N^\dagger)$, where $\mathcal{T}_N = \prod_{j=1}^{j=N} \mathbf{T}_j$, are defined by the corresponding eigenvalues $\lambda_i = e^{\gamma_i}$. All the Lyapunov exponents $\gamma_1 > \gamma_2 > \cdots > \gamma_{4M}$, are computed by a method described in Ref. 13. However, the matrix is not symplectic. Therefore, all $4M$ eigenvalues are computed. Remarkably, except for a small set consisting of large eigenvalues, the rest of the eigenvalues do come in pairs $(\lambda, 1/\lambda)$, as for the symplectic case, within our numerical accuracy. We have no analytical proof of this curious fact. Clearly, large eigenvalues contribute insignificantly to the Pichard-Landauer[12] formula for the conductance, $\sigma_{ab}(B)$:

$$\sigma_{ab}(B) = \frac{e^2}{h} \mathrm{Tr} \sum_{j=1}^{2M} \frac{2}{(\mathcal{T}_N\mathcal{T}_N^\dagger) + (\mathcal{T}_N\mathcal{T}_N^\dagger)^{-1} + 2}. \tag{12}$$

We have chosen M to be 32, smaller than our previous work.[6] The reason for this is that the matrix size including the third-neighbor hopping is larger, $4M \times 4M$ instead of $2M \times 2M$.

We chose N to be of the order of 10^6, as before. This easily led to an accuracy better than 5% for the smallest Lyapunov exponent, γ_i, in all cases.

IV. MAGNETIC BREAKDOWN AND QUANTUM OSCILLATIONS

We compute the conductance as a function of the magnetic field and then Fourier transform the numerical data. This procedure depends of course on the number of data points sampled within a fixed range of the magnetic field, typically between 45 and 60 T. But the location of each peak and the relative ratio of the intensities remain the same. In order to compare the Fourier transformed results, we keep the sampling points fixed in all cases to be 1200.

In Fig. 2, the results for 17% doping for a 5 meV gap and varying degrees of disorder are shown. Both the slow oscillation at a frequency 290 T corresponding to the small hole pocket and 11 700 T corresponding to the large hole pocket, as schematically sketched in Fig. 1 in the extended Brillouin zone, can be seen. Note that partitioning of the spectral weight between the peaks changes as the degree of disorder is increased. If we change the value of the gap to 10 meV, shown in Fig. 3, the overall picture remains the same, although the lower frequency peak is a bit more dominant, as the magnetic breakdown is a little less probable.

For 16% doping, a similar calculation with gaps of 15 and 30 meV also shows some evidence of magnetic breakdown depending on the disorder level, particularly seen in the 15 meV data in Fig. 4. On the other hand, the evidence of magnetic breakdown is much weaker in the 30 meV data shown in Fig. 5. It is important to note that in none of these calculations does one find any evidence of the electron pocket centered at $(\pi,0)$ and its symmetry counterparts, which should correspond roughly to a frequency of 2700 T. This is due in part to the fact that the effect of disorder is stronger on the electron pocket[6] and in part to the fact that at the breakdown junctions transmission coefficient is larger than the reflection coefficient because it entails a large $(\pi/2)$ change in the direction of the momentum; see Fig. 1.

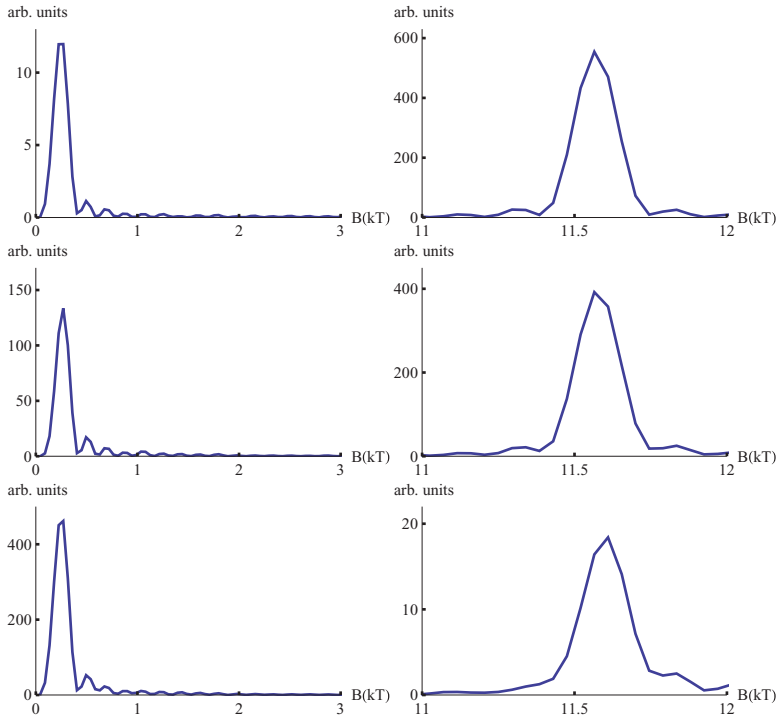

FIG. 2. (Color online) Fourier transform of the conductance oscillations with a smooth background term subtracted. The parameters correspond to 17% doping with a DDW gap of 5 meV and disorder $V_0 = 0.2t$ (row 1), $V_0 = 0.4t$ (row 2), and $V_0 = 0.6t$ (row 3). The horizontal axis is a magnetic field in terms of kilo-Tesla (10^3 T) and the vertical axis is in arbitrary units. The left panels in all cases show the lower frequency component and the right panel the higher-frequency component. Note that there is no evidence of the electron pocket frequency at about $B = 2.7$ kT.

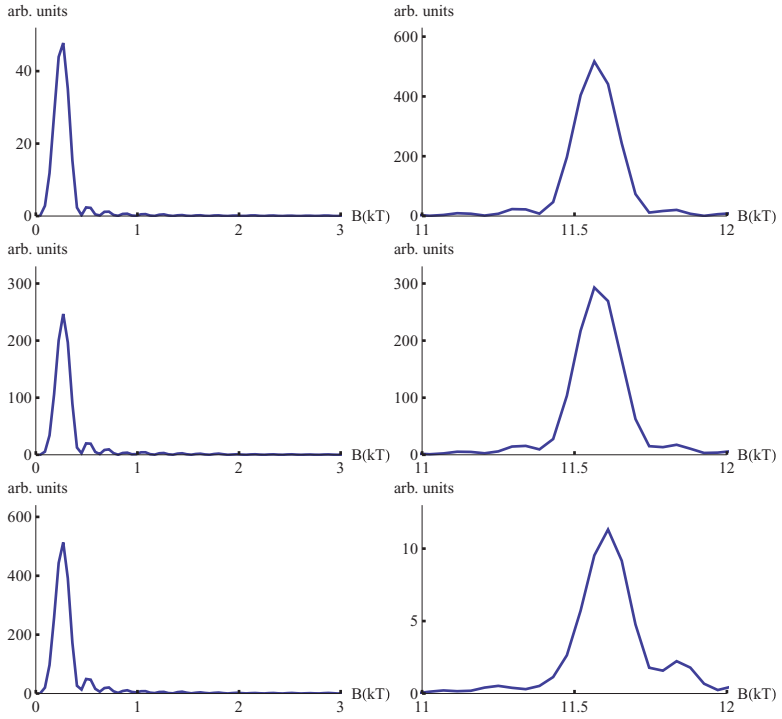

FIG. 3. (Color online) Fourier transform of the conductance oscillations with a smooth background term subtracted. The parameters correspond to 17% doping with a DDW gap of 10 meV and disorder $V_0 = 0.2t$ (row 1), $V_0 = 0.4t$ (row 2), and $V_0 = 0.6t$ (row 3). The horizontal axis is a magnetic field in terms of kilo-Tesla (10^3 T) and the vertical axis is in arbitrary units. The left panels in all cases show the lower frequency component and the right panel the higher frequency component. Note that there is no evidence of the electron pocket frequency at about $B = 2.7$ kT.

V. OSCILLATIONS IN *c*-AXIS RESISTIVITY

The Pichard-Landauer formula was calculated for conductance oscillations in the ab plane, while the actual measurements in NCCO are carried out for the c-axis resistivity. It is therefore necessary to relate the two to compare with experiments. A simple description for a strongly layered material can be obtained by modifying an argument of Kumar and Jayannavar.[14] An applied electric field, E, along the direction perpendicular to the planes will result in a chemical potential difference

$$\Delta\mu = edE, \tag{13}$$

where d is the distance between the two planes of a unit cell. The corresponding current, j_c, is (ε_F is the Fermi energy)

$$j_c = e\,[\Delta\mu g_{2D}(\varepsilon_F, H)]\,\gamma, \tag{14}$$

since $\Delta\mu g_{2D}(\varepsilon_F, H)$ is the number of unoccupied states to which an electron can scatter, while γ is the scattering rate between the planes of a unit cell. Here, we have included a possible oscillatory dependence of the the two-dimensional density of states, $g_{2D}(\varepsilon_F, H)$, that gives rise to Shubnikov–de Haas oscillations in the ab plane. Thus,

$$\rho_c = \frac{E}{j_c} = \frac{1}{e^2 d g_{2D}(\varepsilon_F)\gamma}. \tag{15}$$

There is an implicit assumption: an electron from a given plane makes a transition to a continuum of available states with a finite density at the Fermi surface in the next plane. We are not interested in the Rabi oscillations between two discrete states, a process that cannot lead to resistivity.

The measured ab-plane resistivity is of the order 10 $\mu\Omega$ cm as compared to Ω cm for the c-axis resistivity even at optimum doping,[5] which allows us to make an adiabatic approximation. Because an electron spends much of its time in the plane, making only infrequent hops between the planes, we can adiabatically decouple these two processes. The slower motion along the c axis can be formulated in terms of a 2×2 matrix for each parallel wave vector $\mathbf{k}_\parallel$ after integrating out the planar modes. For simplicity, we are assuming that the c-axis warping is negligible, so there are only two available states of the electron corresponding to its locations in the two planes. The excitations in a plane close to the Fermi surface, $k_\parallel \approx k_{F,\parallel}$, can be approximated by a bosonic heat bath of

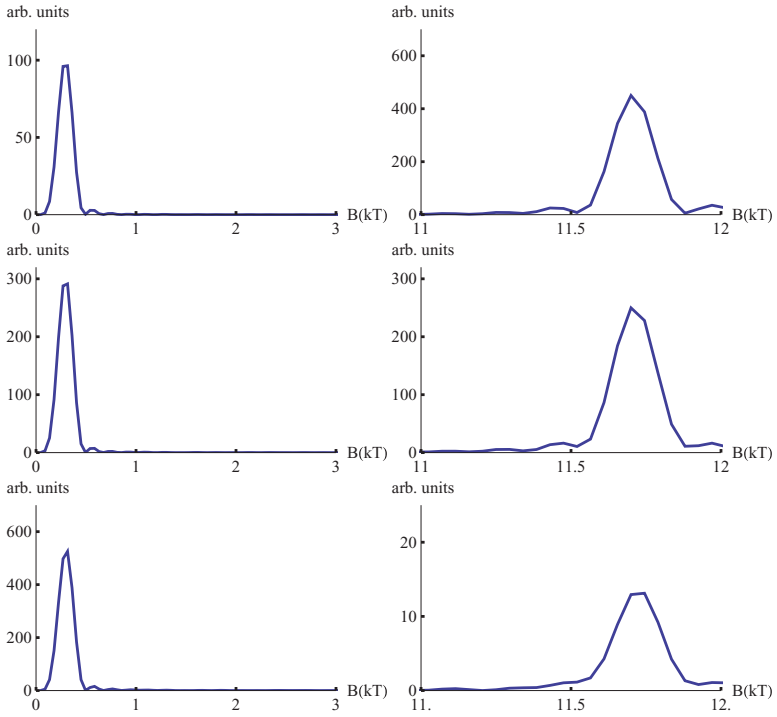

FIG. 4. (Color online) Fourier transform of the conductance oscillations with a smooth background term subtracted. The parameters correspond to 16% doping with a DDW gap of 15 meV and disorder $V_0 = 0.2t$ (row 1), $V_0 = 0.4t$ (row 2), and $V_0 = 0.6t$ (row 3). The horizontal axis is a magnetic field in terms of kilo-Tesla (10^3 T) and the vertical axis is in arbitrary units. The left panels in all cases show the lower frequency component and the right panel the higher frequency component. Note that there is no evidence of the electron pocket frequency at about $B = 2.7$ kT.

particle-hole excitations. In this language, the problem maps onto a two-state Hamiltonian,

$$H = -t_c\sigma_x + \sum_j \hbar\omega_j b_j^\dagger b_j + \frac{\sigma_z}{2}\sum_j f_j(b_j^\dagger + b_j), \quad (16)$$

where σ's are the standard Pauli matrices and t_c is the hopping matrix element between the nearest-neighbor planes. Given the simplification, the sum over $\mathbf{k}_\parallel$ is superfluous, and the problem then maps onto a much studied model of a two-level system coupled to an Ohmic heat bath.[15] The Ohmic nature follows from the fermionic nature of the bath.[16] The effect of the bath on the transition between the planes is summarized by a spectral function,

$$J(\omega) = \frac{\pi}{2}\sum_j f_j^2\delta(\omega - \omega_j). \quad (17)$$

For a fermionic bath, we can choose

$$J(\omega) = \begin{cases} 2\pi\alpha\omega, & \omega \ll \omega_c \\ 0, & \omega \gg \omega_c, \end{cases} \quad (18)$$

where ω_c is a high-frequency cutoff, which is of the order of $\omega_c = 2/\tau_{ab}$, where τ_{ab} is of the order of the planar relaxation time. For a Fermi bath, the parameter α is necessarily restricted to the range $0 \leqslant \alpha \leqslant 1$.[16] Moreover, for coherent oscillations we must have $\alpha < 1/2$.[15] However, we shall leave α as an adjustable parameter, presumably less than or equal to $1/2$ to be consistent with our initial assumptions. While a similar treatment is possible for a non-Fermi liquid,[17] the present discussion is entirely within the Fermi liquid theory.

The quantity γ is the interplanar tunneling rate renormalized by the particle-hole excitations close to the planar Fermi surface and can be easily seen to be[15]

$$\gamma = \frac{2t_c}{\hbar}\left(\frac{2t_c}{\hbar\omega_c}\right)^{\frac{\alpha}{1-\alpha}}. \quad (19)$$

The c-axis resistivity is then

$$\rho_c = \frac{\hbar}{e^2}\frac{1}{d\,g_{2D}(\varepsilon_F, H)\hbar\omega_c}\left(\frac{\hbar\omega_c}{2t_c}\right)^{\frac{1}{1-\alpha}}. \quad (20)$$

This equation can be further simplified by expressing it as a ratio of ρ_c/ρ_{ab}, but this is unnecessary. Two important qualitative points are as follows: ρ_c is far greater than ρ_{ab},

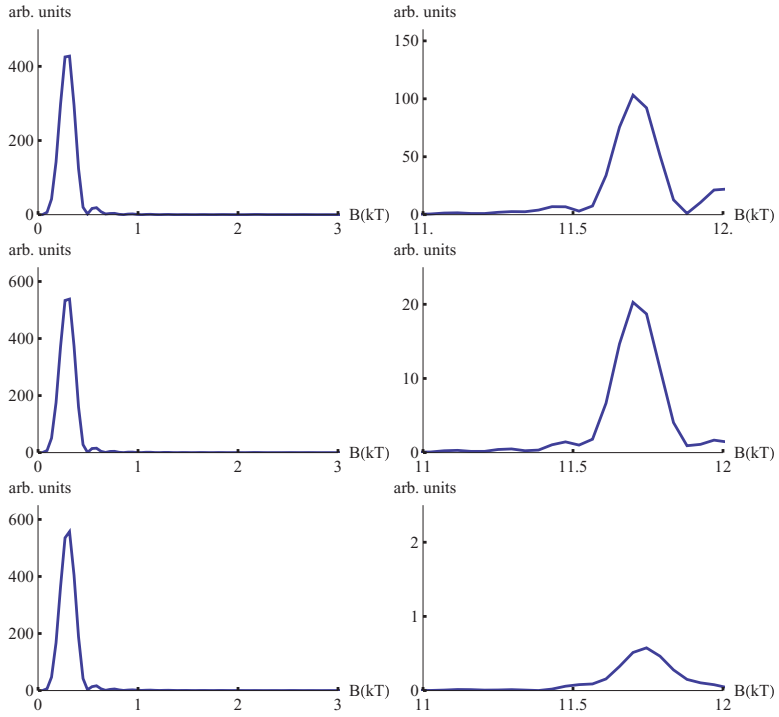

FIG. 5. (Color online) Fourier transform of the conductance oscillations with a smooth background term subtracted. The parameters correspond to 16% doping with a DDW gap of 30 meV and disorder $V_0 = 0.2t$ (row 1), $V_0 = 0.4t$ (row 2), and $V_0 = 0.6t$ (row 3). The horizontal axis is a magnetic field in terms of kilo-Tesla (10^3 T) and the vertical axis is in arbitrary units. The left panels in all cases show the lower frequency component and the right panel the higher frequency component. Note that there is no evidence of the electron pocket frequency at about $B = 2.7$ kT.

and the root of the quantum oscillations of ρ_c is quantum oscillations of the planar density of states.

VI. CONCLUSIONS

We have shown that a qualitatively consistent physical picture for quantum oscillations can be provided with a simple set of assumptions involving reconstruction of the Fermi surface due to density wave order. Although not presented here, we have also noted that even for 15% doping one can observe magnetic breakdown if the gap is small, in the range 20–30 meV. This appears to be consistent with even more recent unpublished experiments.[18] Although the specific order considered here was the DDW, we have shown previously that at the mean-field level, a very similar picture can be provided by a twofold commensurate spin density wave (SDW).[6] Thus, it appeared unnecessary to repeat the same calculations using the SDW order.

In YBCO, studies involving tilted fields seem to rule out a triplet order parameter, hence the SDW.[19] Moreover, from nuclear magnetic resonance (NMR) measurements at high fields, there appears to be no evidence of a static spin density wave order in YBCO.[20] Similarly, there is no evidence of SDW order in fields as high as 23.2 T in $YBa_2Cu_4O_8$,[21] while quantum oscillations are clearly observed in this material.[22] Also, no such evidence of SDW is found up to 44 T in $Bi_2Sr_{2-x}La_xCuO_{6+\delta}$.[23] At present, results from high-field NMR in NCCO do not exist, but measurements are in progress.[24] It is unlikely that such static SDW order will be revealed in these measurements. This conjecture is based on the zero-field neutron-scattering measurements, which indicate a very small spin-spin correlation length in the relevant doping regime.[25] A long-range SDW order cannot appear merely by applying high magnetic fields, which is energetically a weak perturbation even for a 45 T field.[26]

As to singlet order, most likely relevant to the observation of quantum oscillations,[27] a charge density wave is a possibility. This has recently found some support in the high-field NMR measurements in YBCO.[20] As to singlet DDW, there are two neutron scattering measurements that seem to provide evidence for it.[28] However, these measurements have not been confirmed by further independent experiments. However, DDW order should be considerably hidden in NMR involving nuclei at high symmetry points, because the orbital currents should cancel.

A mysterious feature of quantum oscillations in YBCO is the fact that only one type of Fermi pocket is observed. If a twofold commensurate density wave is the mechanism, this will violate the Luttinger sum rule.[3,29] We have previously provided an explanation for this phenomenon in terms of disorder arising from both defects and vortex scattering in the vortex liquid phase.[11] However, the arguments are not unassailable. In contrast, for NCCO, the experimental results are quite consistent with the simple theory discussed above. We have not addressed angle-dependent magnetoresistance oscillations (AMRO) in NCCO, as the data seem to be somewhat anomalous,[8] although within the Fermi liquid framework discussed here it should be possible to address this effect in the future.

The basic question as to why Fermi liquid concepts should apply remains an important unsolved mystery.[30] It is possible that if the state revealed by applying a high magnetic field has a broken symmetry with an order parameter (hence a gap), the low-energy excitations will be quasiparticle-like, not spectra with a branch cut, as in variously proposed strange metal phases. In this respect, the notion of a hidden Fermi liquid may be relevant.[31]

ACKNOWLEDGMENTS

We thank Mark Kartsovnik, Stuart Brown, Marc-Henri Julien, Brad Ramshaw, and Cyril Proust for keeping us updated regarding their latest experiments. In particular, we thank Marc-Henri Julien for sharing with us his unpublished high-field NMR results in YBCO. This work is supported by the NSF under Grant No. DMR-1004520.

APPENDIX: THE DERIVATION OF THE TRANSFER MATRIX

The DDW Hamiltonian in real space is

$$H=\sum_{\mathbf{i}}\epsilon_{\mathbf{i}}c_{\mathbf{i}}^{\dagger}c_{\mathbf{i}}-t\sum_{\langle\mathbf{i},\mathbf{j}\rangle}e^{ia_{\mathbf{i},\mathbf{j}}}c_{\mathbf{i}}^{\dagger}c_{\mathbf{j}}-t'\sum_{\langle\mathbf{i},\mathbf{j}\rangle'}e^{ia_{\mathbf{i},\mathbf{j}}}c_{\mathbf{i}}^{\dagger}c_{\mathbf{j}}-t''\sum_{\langle\mathbf{i},\mathbf{j}\rangle''}e^{ia_{\mathbf{i},\mathbf{j}}}c_{\mathbf{i}}^{\dagger}c_{\mathbf{j}}+\sum_{\mathbf{i}}\frac{iW_0}{4}(-1)^{n+m}c_{\mathbf{i}}^{\dagger}c_{\mathbf{i}+\hat{\mathbf{x}}}-\sum_{\mathbf{i}}\frac{iW_0}{4}(-1)^{n+m}c_{\mathbf{i}}^{\dagger}c_{\mathbf{i}+\hat{\mathbf{y}}}+\text{H.c.} \tag{A1}$$

Here, $e^{ia_{\mathbf{i},\mathbf{j}}}$ is the Peierls phase due to the magnetic field. The summation notations are as follows: $\langle\mathbf{i},\mathbf{j}\rangle$, $\langle\mathbf{i},\mathbf{j}\rangle'$, and $\langle\mathbf{i},\mathbf{j}\rangle''$ imply a sum over nearest-neighbor, next-nearest-neighbor, and the third-nearest-neighbor sites, respectively. For example, with the lattice constant set to unity, $\langle\mathbf{i},\mathbf{j}\rangle$ is satisfied when $\mathbf{i}=\mathbf{j}\pm\hat{\mathbf{x}}$ or $\mathbf{i}=\mathbf{j}\pm\hat{\mathbf{y}}$. Likewise, $\langle\mathbf{i},\mathbf{j}\rangle'$ requires $\mathbf{i}=\mathbf{j}+\hat{\mathbf{x}}\pm\hat{\mathbf{y}}$ or $\mathbf{i}=\mathbf{j}-\hat{\mathbf{x}}\pm\hat{\mathbf{y}}$ and $\langle\mathbf{i},\mathbf{j}\rangle''$ requires $\mathbf{i}=\mathbf{j}\pm2\hat{\mathbf{x}}$ or $\mathbf{i}=\mathbf{j}\pm2\hat{\mathbf{y}}$. Here W_0 is the DDW gap and $\mathbf{i}=(n,m)$. Consider an eigenstate $|\Psi\rangle$ with an energy eigenvalue E: $H|\Psi\rangle=E|\Psi\rangle$, where $|\Psi\rangle=\sum_{\mathbf{i}}\psi(\mathbf{i})|\mathbf{i}\rangle$; the amplitude at a site is $\psi(\mathbf{i})$. Then the Schrödinger equation can be written in terms of the amplitudes $\psi_n(m)$ of the nth slice for all values of $m=1,2,\ldots,M$:

$$\begin{aligned}E\psi_n(m)=\epsilon_{\mathbf{i}}\psi_n(m)&-t[\psi_{n+1}(m)+\psi_{n-1}(m)+e^{-in\phi}\psi_n(m+1)\\&+e^{in\phi}\psi_n(m-1)]-t'[e^{i(-n-\frac{1}{2})\phi}\psi_{n+1}(m+1)\\&+e^{i(n+\frac{1}{2})\phi}\psi_{n-1}(m+1)+e^{i(n+\frac{1}{2})\phi}\psi_{n+1}(m-1)\\&+e^{i(-n-\frac{1}{2})\phi}\psi_{n-1}(m-1)]-t''[\psi_{n+2}(m)+\psi_{n-2}(m)\\&+e^{-i2n\phi}\psi_n(m+2)+e^{i2n\phi}\psi_n(m-2)]\\&+\frac{iW_0}{4}(-1)^{n+m}[\psi_{n+1}(m)+\psi_{n-1}(m)]\\&-\frac{iW_0}{4}(-1)^{n+m}[e^{-in\phi}\psi_n(m+1)+e^{in\phi}\psi_n(m-1)].\end{aligned} \tag{A2}$$

With the periodic boundary condition along the y axis, i.e., $\psi_n(M+1)=\psi_n(1)$, the Schrödinger equation can be expressed as a matrix equation:

$$0=-U_n\psi_{n+2}+A_n\psi_{n+1}+B_n\psi_n+C_n\psi_{n-1}+D_n\psi_{n-2}, \tag{A3}$$

where U_n, A_n, B_n, C_n, and D_n are $M\times M$ matrices defined in the equations following Eq. (3). Now we can solve the Schrödinger equation for ψ_{n+2} to obtain $\psi_{n+2}=U_n^{-1}(A_n\psi_{n+1}+B_n\psi_n+C_n\psi_{n-1}+D_n\psi_{n-2})$. Then the amplitudes at a set of four successive slices, ψ_{n-1} through ψ_{n+2}, can be written in terms of the amplitudes of a previous set of four successive slices, ψ_{n-2} through ψ_{n+1}. Thus, the transfer matrix in the main text follows.

[1] N. Doiron-Leyraud, C. Proust, D. LeBoeuf, J. Levallois, J.-B. Bonnemaison, R. Liang, D. A. Bonn, W. N. Hardy, and L. Taillefer, Nature (London) **447**, 565 (2007).

[2] S. C. Riggs, O. Vafek, J. B. Kemper, J. Betts, A. Migliori, W. N. Hardy, R. Liang, D. A. Bonn, and G. Boebinger, Nat. Phys. **7**, 332 (2011).

[3] S. Chakravarty, Science **319**, 735 (2008); S. Chakravarty and H.-Y. Kee, Proc. Natl. Acad. Sci. USA **105**, 8835 (2008); I. Dimov, P. Goswami, X. Jia, and S. Chakravarty, Phys. Rev. B **78**, 134529 (2008); A. J. Millis and M. R. Norman, *ibid.* **76**, 220503 (2007); H. Yao, D.-H. Lee, and S. A. Kivelson, Phys. Rev. B **84**, 012507 (2011).

[4] T. Helm, M. V. Kartsovnik, M. Bartkowiak, N. Bittner, M. Lambacher, A. Erb, J. Wosnitza, and R. Gross, Phys. Rev. Lett. **103**, 157002 (2009).

[5] N. P. Armitage, P. Fournier, and R. L. Green, Rev. Mod. Phys. **82**, 2421 (2009).

[6] J. Eun, X. Jia, and S. Chakravarty, Phys. Rev. B **82**, 094515 (2010).

[7] T. Helm, M. V. Kartsovnik, I. Sheikin, M. Bartkowiak, F. Wolff-Fabris, N. Bittner, W. Biberacher, M. Lambacher, A. Erb, J. Wosnitza, and R. Gross, Phys. Rev. Lett. **105**, 247002 (2010).

[8] M. V. Kartsovnik *et al.*, New J. Phys. **13**, 015001 (2011).

[9] S. Chakravarty, R. B. Laughlin, D. K. Morr, and C. Nayak, Phys. Rev. B **63**, 094503 (2001).

[10]E. Pavarini, I. Dasgupta, T. Saha-Dasgupta, O. Jepsen, and O. K. Andersen, Phys. Rev. Lett. **87**, 047003 (2001).
[11]X. Jia, P. Goswami, and S. Chakravarty, Phys. Rev. B **80**, 134503 (2009).
[12]J. L. Pichard and G. André, Europhys. Lett. **2**, 477 (1986); D. S. Fisher and P. A. Lee, Phys. Rev. B **23**, 6851 (1981).
[13]B. Kramer and M. Schreiber, in *Computational Physics*, edited by K. H. Hoffmann and M. Schreiber (Springer, Berlin, 1996), p. 166.
[14]N. Kumar and A. M. Jayannavar, Phys. Rev. B **45**, 5001 (1992).
[15]S. Chakravarty and A. J. Leggett, Phys. Rev. Lett. **52**, 5 (1984); A. J. Leggett, S. Chakravarty, A. T. Dorsey, M. P. A. Fisher, A. Garg, and W. Zwerger, Rev. Mod. Phys. **59**, 1 (1987).
[16]L.-D. Chang and S. Chakravarty, Phys. Rev. B **31**, 154 (1985).
[17]S. Chakravarty and P. W. Anderson, Phys. Rev. Lett. **72**, 3859 (1994).
[18]M. V. Kartsovnik (unpublished).
[19]B. J. Ramshaw, B. Vignolle, R. Liang, W. N. Hardy, C. Proust, and D. A. Bonn, Nat. Phys. **7**, 234 (2011); S. E. Sebastian, N. Harrison, M. M. Altarawneh, F. F. Balakirev, C. H. Mielke, R. Liang, D. A. Bonn, W. N. Hardy, and G. G. Lonzarich, e-print arXiv:1103.4178v1 (cond-mat).
[20]T. Wu, H. Mayaffre, S. Kramer, M. Horvatic, C. Berthier, W. Hardy, R. Liang, D. Bonn, and M.-H. Julien (unpublished).
[21]G.-q. Zheng, W. G. Clark, Y. Kitaoka, K. Asayama, Y. Kodama, P. Kuhns, and W. G. Moulton, Phys. Rev. B **60**, R9947 (1999).
[22]E. A. Yelland, J. Singleton, C. H. Mielke, N. Harrison, F. F. Balakirev, B. Dabrowski, and J. R. Cooper, Phys. Rev. Lett. **100**, 047003 (2008); A. F. Bangura, J. D. Fletcher, A. Carrington, J. Levallois, M. Nardone, B. Vignolle, P. J. Heard, N. Doiron-Leyraud, D. LeBoeuf, L. Taillefer, S. Adachi, C. Proust, and N. E. Hussey, *ibid.* **100**, 047004 (2008).
[23]S. Kawasaki, C. Lin, P. L. Kuhns, A. P. Reyes, and G.-q. Zheng, Phys. Rev. Lett. **105**, 137002 (2010).
[24]S. E. Brown (unpublished).
[25]E. M. Motoyama, G. Yu, I. M. Vishik, O. P. Vajk, P. K. Mang, and M. Greven, Nature (London) **445**, 186 (2007).
[26]H. K. Nguyen and S. Chakravarty, Phys. Rev. B **65**, 180519 (2002).
[27]D. Garcia-Aldea and S. Chakravarty, Phys. Rev. B **82**, 184526 (2010); M. R. Norman and J. Lin, *ibid.* **82**, 060509 (2010); R. Ramazashvili, Phys. Rev. Lett. **105**, 216404 (2010).
[28]H. A. Mook, P. Dai, S. M. Hayden, A. Hiess, J. W. Lynn, S. H. Lee, and F. Doğan, Phys. Rev. B **66**, 144513 (2002); H. A. Mook, P. Dai, S. M. Hayden, A. Hiess, S. H. Lee, and F. Doğan, *ibid.* **69**, 134509 (2004).
[29]J. M. Luttinger, Phys. Rev. **119**, 1153 (1960); A. V. Chubukov and D. K. Morr, Phys. Rep. **288**, 355 (1997); B. L. Altshuler, A. V. Chubukov, A. Dashevskii, A. M. Finkel'stein, and D. K. Morr, Europhys. Lett. **41**, 401 (1998).
[30]S. Chakravarty, Rep. Prog. Phys. **74**, 022501 (2011).
[31]P. A. Casey and P. W. Anderson, Phys. Rev. Lett. **106**, 097002 (2011).

Quantum oscillations in $YBa_2Cu_3O_{6+\delta}$ from an incommensurate d-density wave order

Jonghyoun Eun, Zhiqiang Wang, and Sudip Chakravarty
Department of Physics and Astronomy, University of California Los Angeles, Los Angeles, California 90095-1547, USA
(Dated: March 5, 2012)

We consider quantum oscillation experiments in $YBa_2Cu_3O_{6+\delta}$ from the perspective of an incommensurate Fermi surface reconstruction using an exact transfer matrix method and the Pichard-Landauer formula for the conductivity. The specific density wave order considered is a period-8 d-density wave in which the current density is unidirectionally modulated. The current modulation is also naturally accompanied by a period-4 site charge modulation in the same direction, which is consistent with recent magnetic resonance measurements. In principle Landau theory also allows for a period-4 bond charge modulation, which is not discussed, but should be simple to incorporate in the future. This scenario leads to a natural, but not a unique, explanation of why only oscillations from a single electron pocket is observed, and a hole pocket of roughly twice the frequency as dictated by two-fold commensurate order, and the corresponding Luttinger sum rule, is not observed. However, it is possible that even higher magnetic fields will reveal a hole pocket of half the frequency of the electron pocket or smaller. This may be at the borderline of achievable high field measurements because at least a few complete oscillations have to be clearly resolved.

I. INTRODUCTION

The discovery of quantum oscillations[1] in the Hall coefficient (R_H) of hole-doped high temperature superconductor $YBa_2Cu_3O_{6+\delta}$ (YBCO) in high magnetic fields approximately between $35 - 62$ T was an important event.[2] Although the original measurements were performed in the underdoped regime, close to 10% hole doping, later measurements have also revealed clear oscillations for $YBa_2Cu_4O_8$ (Y248), which corresponds to about 14% doping.[3,4] Fermi surface reconstruction due to a density wave order that could arise if superconductivity is "effectively destroyed" by high magnetic fields has been a promising focus of attention.[5–10] Similar quantum oscillations in the c-axis resistivity in $Nd_{2-x}Ce_xCuO_4$ (NCCO)[11] have been easier to interpret in terms of a two-fold commensurate density wave order, even quantitatively, including magnetic breakdown effects.[12]

At this time, in YBCO, there appears to be no general agreement about the precise nature of the translational symmetry breaking. A pioneering idea invoked an order corresponding to period-8 anti-phase spin stripes.[5] The emphasis there was to show how over a reasonable range of parameters the dominant Fermi pockets are electron pockets, thus explaining the observed negative Hall coefficient. At around the same time one of us suggested a two-fold commensurate d-density wave (DDW) order that could also explain the observations.[6]There are several reasons for such a choice. One of them is that the presence of both hole and electron pockets with differing scattering rates leads to a natural explanation[6] of oscillations of R_H. An incommensurate period-8 DDW was also considered.[7] Fermi surfaces resulting from this order are very similar to those due to spin stripes. The lack of Luttinger sum rule and a multitude of possible reconstructed Fermi surfaces appeared to have little constraining power in a Hartree-Fock mean field theory. However, since then many experiments that indicate the importance of stripe physics[13] and even possible unidirectional charge order have led us to reconsider the period-8 DDW.

We enumerate below further motivation for this reconsideration.

- Tilted field measurements have revealed spin zeros in quantum oscillations, which indicate that the symmetry breaking order parameter is a singlet instead of a triplet.[14,15] The chosen order parameter is therefore likely to be a singlet particle-hole condensate rather than a triplet. The nuclear magnetic resonance (NMR) in high fields indicate that there is no spin order but a period-4 charge order that develops at low temperatures.[16]

- As long as the CuO-plane is square planar, the currents induced by the DDW cannot induce net magnetic moment to couple to the nuclei in a NMR measurement. Any deviation from the square planar character could give rise to a NMR signal.[17] To the extent these deviations are small the effects will be also small. Thus the order is very effectively hidden.[18,19]

- While commensurate models can explain measurements in NCCO, it appears to fail to explain the measurements in YBCO. Luttinger sum rule leads to a concommitatnt hole pocket with an oscillation frequency roughly about twice the frequency of the electron pocket (~ 500 T). Despite motivated search no such frequency has been detected. In contrast, for incommensurate period-8 DDW the hole pockets can be quite *small* for a range of parameters. In order to convincingly detect such an oscillation, it is necessary to perform experiments in much higher fields than currently practiced. This may be a resolution of the nonobervation of the hole pocket. However, a tantalizing evidence of a frequency (250 T) has been reported in a recent $85T$ measurement,[20] but its confirmation will require further experiments.

In Sec. II we describe our model, while in Sec. III we outline the transfer matrix calculation of the conductivity. In Sec.

IV, we describe our results, most importantly the quantum oscillation spectra. The final section, V, contains a discussion and an overall outlook.

II. THE MODEL

A. Band structure

The parametrization of the single particle band structure for YBCO from angle resolved photoemission spectroscopy (ARPES) is not entirely straightforward because cleaving at any nominal doping leads to an overdoped surface. Nonetheless an interesting attempt was made to reduce the doping by a potassium overlayer.[21] Further complications arise from bilayer splitting and chain bands. Nonetheless, the inferred band structure appears to be similar to other cuprates where ARPES is a more controlled probe.[22] Here we shall adopt a dispersion that has become common and has its origin in a local density approximation (LDA) based calculation,[23] which is

$$\begin{aligned}\epsilon_{\mathbf{k}} = &-2t(\cos k_x + \cos k_y) + 4t' \cos k_x \cos k_y \\ &- 2t''(\cos 2k_x + \cos 2k_y).\end{aligned} \tag{1}$$

The band parameters are chosen to be $t = 0.15eV$, $t' = 0.32t$, and $t'' = 0.5t'$.[23] The only difference with the conventional LDA band structure is a rough renormalization of t (from $0.38eV$ to $0.15eV$), which is supported by many ARPES experiments that find that LDA overestimates the bandwidth. A more recent ARPES measurement on thin films paints a somewhat more complex picture.[24]

B. Incommensurate DDW without disorder

An Ansatz for period-eight incommensurate DDW[7] involves the wave vector $\mathbf{Q} = (\frac{\pi}{a}, \frac{\pi}{a}) - \frac{\pi}{a}(2\eta, 0) = \frac{\pi}{a}(\frac{3}{4}, 1)$ for $\eta = 1/8$. With the 8-component spinor defined by $\chi^\dagger_{\mathbf{k}} = (c_{\mathbf{k}\uparrow,\alpha}, c^\dagger_{\mathbf{k}+\mathbf{Q},\alpha}, c^\dagger_{\mathbf{k}+2\mathbf{Q},\alpha}, \dots c^\dagger_{\mathbf{k}+8\mathbf{Q}})$, the Hamiltonian without disorder can be written as

$$\mathcal{H} = \sum_{\mathbf{k},\alpha} \chi^\dagger_{\mathbf{k}\alpha} Z_{\mathbf{k},\alpha} \chi_{\mathbf{k}\alpha} \tag{2}$$

The up and down spin sector eigenvalues merely duplicate each other, and we can consider simply one of them:

$$Z_{\mathbf{k}} = \begin{pmatrix} \epsilon_{\mathbf{k}} - \mu & iG_{\mathbf{k}} & V_c & 0 & 0 & 0 & V_c & -iG_{\mathbf{k}+7\mathbf{Q}} \\ \text{c.c} & \epsilon_{\mathbf{k}+\mathbf{Q}} - \mu & iG_{\mathbf{k}+\mathbf{Q}} & V_c & 0 & 0 & 0 & V_c \\ V_c & \text{c.c} & \epsilon_{\mathbf{k}+2\mathbf{Q}} - \mu & iG_{\mathbf{k}+2\mathbf{Q}} & V_c & 0 & 0 & 0 \\ 0 & V_c & \text{c.c} & \epsilon_{\mathbf{k}+3\mathbf{Q}} - \mu & iG_{\mathbf{k}+3\mathbf{Q}} & V_c & 0 & 0 \\ 0 & 0 & V_c & \text{c.c} & \epsilon_{\mathbf{k}+4\mathbf{Q}} - \mu & iG_{\mathbf{k}+4\mathbf{Q}} & V_c & 0 \\ 0 & 0 & 0 & V_c & \text{c.c} & \epsilon_{\mathbf{k}+5\mathbf{Q}} - \mu & iG_{\mathbf{k}+5\mathbf{Q}} & V_c \\ V_c & 0 & 0 & 0 & V_c & \text{c.c} & \epsilon_{\mathbf{k}+6\mathbf{Q}} - \mu & iG_{\mathbf{k}+6\mathbf{Q}} \\ iG_{\mathbf{k}+7\mathbf{Q}} & V_c & 0 & 0 & 0 & V_c & \text{c.c} & \epsilon_{\mathbf{k}+7\mathbf{Q}} - \mu \end{pmatrix}, \tag{3}$$

where $G_{\mathbf{k}} = (W_{\mathbf{k}} - W_{\mathbf{k}+\mathbf{Q}})/2$, and the DDW gap is $W_{\mathbf{k}} = \frac{W_0}{2}(\cos k_x - \cos k_y)$. On symmetry grounds, one can quite generally expect that an incommensurate DDW with wave vector $\mathbf{Q}$ will induce a charge density wave (CDW) of wave vector $2\mathbf{Q}$.[18] This fact is taken into account by explicitly incorporating a period-4 CDW by introducing the real matrix elements V_c. The chemical potential μ and the DDW gap amplitude W_0 can be adjusted to give the desired quantum oscillation frequency of the electron pocket as well as the doping level. The Fermi surfaces corresponding to the spectra of Eq. (2) (an example is shown in Fig. 1) are not essentially different from the mean field theory of $1/8$ magnetic antiphase stripe order.[5] This higher order commensuration generically produces complicated Fermi surfaces, involving open orbits, hole pockets, and electron pockets.

To picture the current modulation and to define the order parameter of period-8 DDW in the real space Hamiltonian we need to calculate $\langle c^\dagger_{\mathbf{R}'} c_{\mathbf{R}} \rangle$ for $\mathbf{R}' \neq \mathbf{R}$. We get, correcting here a mistake in Ref. 7,

$$\begin{aligned}\langle c^\dagger_{\mathbf{R}'} c_{\mathbf{R}} \rangle &= \frac{1}{N} \sum_{\mathbf{k}'\mathbf{k}} \langle c^\dagger_{\mathbf{k}'} c_{\mathbf{k}} \rangle \exp\left[-i(\mathbf{k}' \cdot \mathbf{R}' - \mathbf{k} \cdot \mathbf{R})\right] \\ &= \pm \frac{iW_0}{2} (-1)^{n'+m'} \widetilde{V}_{\mathbf{R}',\mathbf{R}},\end{aligned} \tag{4}$$

where $\mathbf{R}' = (m'a, n'a)$, and $\widetilde{V}_{\mathbf{R}',\mathbf{R}}$ is

$$\begin{aligned}\widetilde{V}_{\mathbf{R}',\mathbf{R}} = &\left[\frac{1 + \cos 2\pi\eta}{2}(\delta_{\mathbf{R}',\mathbf{R}+a\hat{\mathbf{x}}} + \delta_{\mathbf{R}',\mathbf{R}-a\hat{\mathbf{x}}}) \right. \\ &\left. - (\delta_{\mathbf{R}',\mathbf{R}+a\hat{\mathbf{y}}} + \delta_{\mathbf{R}',\mathbf{R}-a\hat{\mathbf{y}}})\right] \cos 2m'\pi\eta \\ &+ \frac{\sin 2\pi\eta \sin 2m'\pi\eta}{2}(\delta_{\mathbf{R}',\mathbf{R}+a\hat{\mathbf{x}}} - \delta_{\mathbf{R}',\mathbf{R}-a\hat{\mathbf{x}}}).\end{aligned} \tag{5}$$

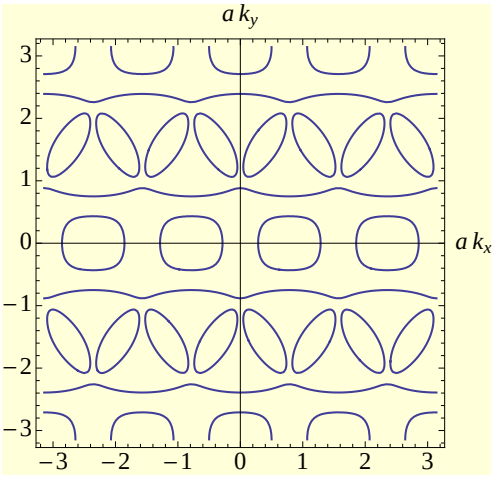

FIG. 1. Reconstructed Fermi surafces with $\mathbf{Q} = \frac{\pi}{a}(\frac{3}{4}, 1)$, $W_0 = 0.65t$, $V_c = 0.05t$, and $\mu = -0.83t$. There are electron pockets, hole pockets and open orbits. The electron pocket frequency corresponds to 530T and the hole pockets to 280T. The doping corresponds to 12.46%. Note that the figure is shown in the extended BZ for clarity.

The current pattern is then

$$\begin{aligned} J_{\mathbf{R}',\mathbf{R}} &= i[\langle c^\dagger_{\mathbf{R}'} c_{\mathbf{R}}\rangle - \langle c^\dagger_{\mathbf{R}} c_{\mathbf{R}'}\rangle] \\ &= -W_0(-1)^{n'+m'}\widetilde{V}_{\mathbf{R}',\mathbf{R}}, \end{aligned} \tag{6}$$

which is drawn in Fig. 2. The incommensurate d-density wave order parameter is proportional to

$$\widetilde{W}_{\mathbf{R}',\mathbf{R}} = \frac{\mathrm{i}W_0}{2}(-1)^{n'+m'}\widetilde{V}_{\mathbf{R}',\mathbf{R}}. \tag{7}$$

C. The real space Hamiltonian including disorder

In real space, the Hamiltonian in the presence of both disorder and magnetic field is

$$\begin{aligned} H = &\sum_{\mathbf{R}} [V(\mathbf{R}) + 2V_c\cos(\pi m/2)]\, c^\dagger_{\mathbf{R}} c_{\mathbf{R}} \\ &+ \sum_{\mathbf{R}',\mathbf{R}} t_{\mathbf{R}',\mathbf{R}}\, \mathrm{e}^{\mathrm{i}a_{\mathbf{R}',\mathbf{R}}} c^\dagger_{\mathbf{R}'} c_{\mathbf{R}} \\ &+ \sum_{\mathbf{R}',\mathbf{R}} \widetilde{W}_{\mathbf{R}',\mathbf{R}}\, \mathrm{e}^{\mathrm{i}a_{\mathbf{R}',\mathbf{R}}} c^\dagger_{\mathbf{R}'} c_{\mathbf{R}} + h.c. \end{aligned} \tag{8}$$

Here $t_{\mathbf{R}',\mathbf{R}}$ defines the band structure: the nearest neighbor, the next nearest neighbor, and the third nearest neighbor hopping terms: t, t', t''. And $2V_c\cos(\frac{\pi}{2}m)$ is responsible for the period-four charge stripe order, where m is $\mathbf{R}\cdot\hat{x}/a$ and a is lattice spacing. We include correlated disorder in the form[25]

$$V(\mathbf{R}) = \frac{g_V}{2\pi l_D^2}\int d\mathbf{x}\, e^{-\frac{|\mathbf{R}-\mathbf{x}|^2}{2l_D^2}}\, u(\mathbf{x}), \tag{9}$$

where l_D is the disorder correlation length and the disorder averages are $\langle u(\mathbf{x})\rangle = 0$ and $\langle u(\mathbf{x})u(\mathbf{y})\rangle = \delta(\mathbf{x}-\mathbf{y})$; the disorder intensity is set by g_V.

While white noise disorder seems to be more appropriate for NCCO with intrinsic disorder, correlated disorder may be more relevant to relatively clean YBCO samples in the range of well ordered chain compositions. Thus, here we shall focus on correlated disorder. A constant perpendicular magnetic field B is included via the Peierls phase factor $a_{\mathbf{R}',\mathbf{R}} = \frac{e}{\hbar c}\int_{\mathbf{R}}^{\mathbf{R}'}\mathbf{A}\cdot\mathrm{dl}$, where $\mathbf{A} = (0, -Bx, 0)$ is the vector potential in the Landau gauge; the lattice vector $\mathbf{R}' = (m'a, n'a)$ is defined by an arbitrary set of integers.

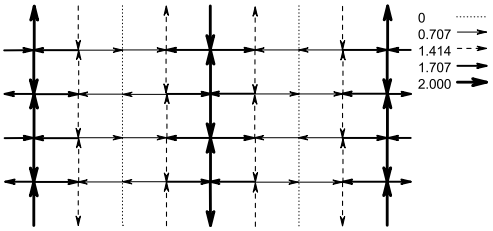

FIG. 2. Current pattern for $\mathbf{Q} = (\frac{3\pi}{4a}, \frac{\pi}{a})$. The relative magnitudes of the currents are depicted by the arrows in the legend. Note the antiphase domain wall structure.

III. THE TRANSFER MATRIX METHOD

The transfer matrix technique is a powerful method to compute conductance oscillations. It requires neither quasiclassical approximation nor *ad hoc* broadening of the Landau level to incorporate the effect of disorder. Various models of disorder, both long and short-ranged, can be studied *ab initio*. The mean field Hamiltonian, being a quadratic non-interacting Hamiltonian, leads to a Schrödinger equation for the site amplitudes, which is then recast in the form of a transfer matrix; the derivation has been discussed in detail previously.[12,25] The conductance is then calculated by a formula that is well known in the area of mesoscopic physics, the Pichard-Landauer formula.[26] This yields Shubnikov-de Haas oscillations of the ab-plane resistivity, ρ_{ab}.

We consider a quasi-1D system, $N \gg M$, with a periodic boundary condition along y-direction. Here Na is the length in the x-direction and Ma is the length in the y-direction. Let $\Psi_n = (\psi_{n,1}, \psi_{n,2}, \ldots, \psi_{n,M})^T$, $n = 1, \ldots N$, be the amplitudes on the slice n for an eigenstate with a given energy. Then the amplitudes between the successive slices depending on the Hamiltonian must form a given transfer matrix, $\mathbb{T}$.

The complete set of Lyapunov exponents, γ_i, of $\lim_{N\to\infty}(\mathcal{T}_N\mathcal{T}_N^\dagger)$, where $\mathcal{T}_N = \prod_{j=1}^{j=N} \mathbb{T}_j$ determine the conductance, $\sigma_{ab}(B)$ from the Pichard-Landauer formula:

$$\sigma_{ab}(B) = \frac{e^2}{h}\mathrm{Tr}\sum_{j=1}^{2M}\frac{2}{(\mathcal{T}_N\mathcal{T}_N^\dagger) + (\mathcal{T}_N\mathcal{T}_N^\dagger)^{-1} + 2}. \quad (10)$$

In this work we have chosen $M = 30$ and N of the order of 10^5. This guaranteed 4% accuracy of the smallest Lyapunov exponent. Note that at each step we have to invert a $4M \times 4M$ matrix and numerical errors prohibit much larger values of M.

IV. RESULTS

A. Specific heat without disorder

The coefficient of the linear specific heat is

$$\gamma = \frac{\pi^2}{3}k_B^2\,\rho(0). \quad (11)$$

The density of states $\rho(\omega)$ measured with respect to the Fermi energy can be easily computed by taking into account all eight bands in the irreducible part of the Full Brillouin zone and a factor of 2 for spin. A Lorentzian broadening of the δ-functions was used in computing the density of states. Although this is useful for numerical computation, the smoothing is a rough way of incorporating the effect of disorder on the density of states.

For a single CuO-layer we get,

$$\gamma \approx 5.4\frac{mJ}{mole.K^2}, \quad (12)$$

where we have used the density of states at the Fermi energy from numerical calculation to be approximately 2.3 states/eV, as shown in the Figure 3. Including both layers $\gamma = 2 \times 5.4 = 10.8\frac{mJ}{mole.K^2}$, approximately a factor of 2 larger than the observed $5\frac{mJ}{mole.K^2}$ at $45T$.[27]

B. Charge modulation without disorder

Before we carry out an explicit calculation it is useful to make a qualitative estimate. For $V_c = 0.05t$, the total charge gap is to $4V_c = 0.2t$. In order to convert to modulation of the charge order parameter, we have to divide by a suitable coupling constant. In high temperature superconductors, all important coupling constants are of the order bandwidth, which is $8t = 1.2eV$. Taking this as a rough estimate, we deduce that the charge modulation is $0.025e$, expressed in terms of electronic charge.

To explicitly calculate charge modulation at a site, we diagonalize the 8×8 Hamiltonian matrix $Z(k_x, k_y)$ for each $\mathbf{k}$ in the reduced Brillouin zone (RBZ). We get 8 eigenvalues and the corresponding eigenvectors: E_{n,k_x,k_y} and ψ_{n,k_x,k_y}

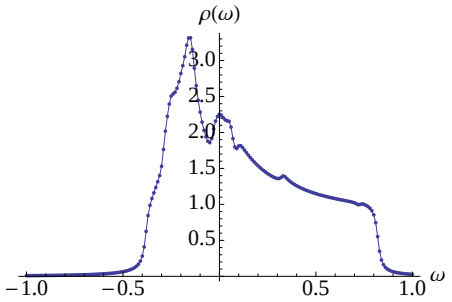

FIG. 3. Total density of states, $t = 0.15$, including eight bands in the reduced Brillouin zone per layer. The horizontal axis is in terms of electron volts and the vertical axis is a pure number, that is, the number of states. The rounding at the tails is due to the Lorentzian broadening of the δ-functions by $\Gamma = 0.1t$. The remaining parameters are the same as in Fig. 1. Further smoothing will reduce the density of states at the Fermi energy and lower the value of γ.

for $n = 1, 2, ..., 8$. The eigenvector ψ_{n,k_x,k_y} has eight components of the form:

$$\psi_{n,k_x,k_y} = (\alpha_{n,k_x,k_y}(1), \alpha_{n,k_x,k_y}(2), ..., \alpha_{n,k_x,k_y}(8)) \quad (13)$$

Then the wave function in the real space for each state $\{n, k_x, k_y\}$ is

$$\psi_{n,k_x,k_y}(\mathbf{R}) = \sum_{j=1}^{8}\alpha_{n,k_x,k_y}(j)\frac{1}{\sqrt{N}}\exp i(\mathbf{k} + (j-1)\mathbf{Q})\cdot\mathbf{R} \quad (14)$$

So, by definition, the local number density is

$$n(\mathbf{R}) = 2 \times {\sum_{n,k_x,k_y}}' \left|\psi_{n,k_x,k_y}(\mathbf{R})\right|^2 \quad (15)$$

Here the prime in the sum means that all *occupied states with energy below the chemical potential* are considered. The factor of 2 is for spin and the summation over k_x, k_y is performed in the RBZ. For different parameter sets the numerical results are:

- Parameter set 1
  $W_0 = 0.71t, V_c = 0.05t, \mu = -0.78t, x = 11.73\%$
  Averaged number density of electron is $n = 0.894$ per site, while the estimated deviation is about $\delta n = 0.059$ per site. So $\delta n/n = 6.6\%$.

- Parameter set 2
  $W_0 = 0.65t, V_c = 0.05t, \mu = -0.83t, x = 12.46\%$
  Averaged number density of electron is: $n = 0.893$ per site, while the estimated deviation is about $\delta n = 0.062$ per site. So $\delta n/n = 6.9\%$.

Of course, for both cases, the period of the CDW modulation is $4a$, where a is the lattice spacing. It is also interesting to

calculate the ratio of the modulation of the *local density of states* to the average density of states at the *Fermi energy*; we find $\delta\rho(\mu)/\rho(\mu) \approx 13 - 15\%$ depending on the parameters. As pointed out in Ref. 10, this leads to an estimate of the corresponding variation of the Knight shift.

C. Oscillation spectra in the presence of correlated disorder

Previously it was found from the consideration of $1/8$ magnetic antiphase stripe order that there is a remarkable variety of possible Fermi surface reconstructions depending on the choice of parameters.[5] This is also true for the incommensurate period-8 DDW. In contrast, two-fold commensurate DDW order leads to much lesser variety. While this is more satisfying, period-4 charge modulation observed in NMR measurements[16] and the non-existence of the larger hole pocket commensurate with the Luttinger sum rule have forced us to take seriously the period-8 DDW. This requires a judicious choice of parameters of the model.

Although we cannot constrain the parameters uniquely, we have used a number of guiding principles. First, disorder was chosen to be correlated with a length scale ℓ_D smaller than the transverse width of the strip, Ma. Since the YBCO samples studied appear to have lesser degree of disorder than the intrinsic disorder of NCCO, the white noise disorder did not appear sensible. Because the experimentally measured charge modulation in NMR is $0.03 \pm 0.01e$, it is necessary to keep V_c small enough to be consistent with experiments. A value of V_c in the neighborhood of $0.05t$ seemed reasonable. Of course, this could be adjusted to agree precisely with experiments, but this would not have been very meaningful.

The band structure parameter t was chosen to be $0.15eV$ as opposed to LDA value of $0.38eV$. Although reliable ARPES measurements are not available for YBCO, measurements in other cuprates have indicated that the bandwidth is renormalized by at least a factor of 2. Had we chosen $t = 0.38eV$, the agreement with specific heat measurements would have been essentially perfect, but we could not see any justification for this. The parameters t'/t and t''/t' are same as the commonly used LDA values, as the shape of the Fermi surface in most cases appear to be given correctly by LDA. We searched the remaining parameters, μ, g_V and W_0, extensively. There are a number of issues worth noting. Oscillation spectra hardly ever show any substantial evidence of harmonics, which should be used as a constraining factor. Moreover, as we believe that it is the electron pocket that is dominant in producing negative R_H, it is necessary that we do not employ parameters that wipe out the electron pocket altogether. The coexistence of electron and hole pockets give a simple explanation of the oscillations of R_H as a function of the magnetic field. We generically found hole pocket frequencies in the range $150 - 300$T. This is one of our crucial observations. It implies that to resolve clearly such a slow frequency, one must go to much higher fields than are currently possible. We argue that this may be a plausible reason why the hole pocket has not been observed except for one experiment which goes up to 85T; in this experiment some evidence of a 250T frequency is observed.[20]

A further constraining fact is that no evidence of magnetic breakdown is observed in YBCO, while in NCCO it is clearly present. This implies that our parameters should be consistent with this fact. The DDW gap and the disorder level are consistent with the observed data. Overall we find satisfactory consistency with doping levels between $11 - 12.5\%$ within our calculational scheme. Lower doping levels produce less satisfactory agreement, but can be made better with further adjustment of parameters, but we have avoided fine tuning as much as possible. The broad brush picture can already be seen in the oscillation spectra in Figs. 4, 5, 6, and 7. Two general trends are that electron pockets dominate at higher doping levels within the range we have checked, and an increase in disorder intensity reduces the intensity of the Fourier spectra of the electron pockets. A few harmonics are still present.

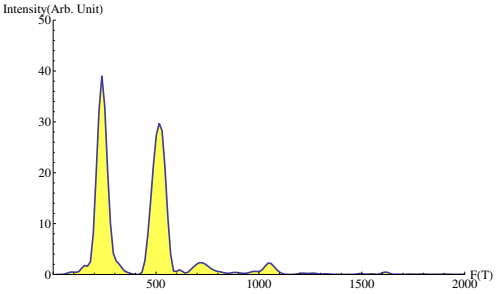

FIG. 4. Fourier transform of the oscillation spectra after a background subtraction with a cubic polynomial. $W_0 = 0.71t$, $V_c = 0.05t$, $\mu = -0.78t$, $M = 30\ a$, $N = 10^5\ a$, $\ell_D = 8\ a$, $g_V = 0.1t$. Doping is 11.73%.

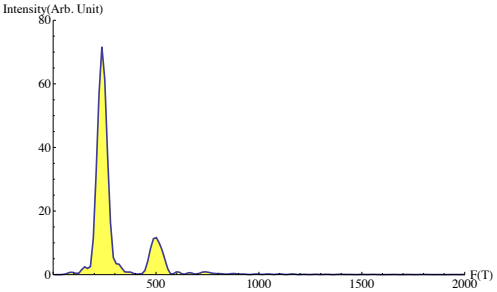

FIG. 5. Fourier transform of the oscillation spectra after a background subtraction with a cubic polynomial. $W_0 = 0.71t$, $V_c = 0.05t$, $\mu = -0.78t$, $M = 30\ a$, $N = 10^5\ a$, $\ell_D = 8\ a$, $g_V = 0.3t$. Doping is 11.73%.

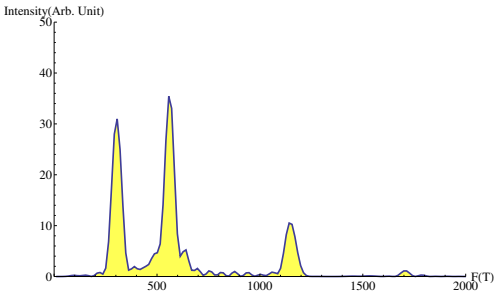

FIG. 6. Fourier transform of the oscillation spectra after a background subtraction with a cubic polynomial. $W_0 = 0.65t$, $V_c = 0.05t$, $\mu = -0.83t$, $M = 30\ a$, $N = 10^5\ a$, $\ell_D = 8\ a$, $g_V = 0.1t$. Doping is 12.46%.

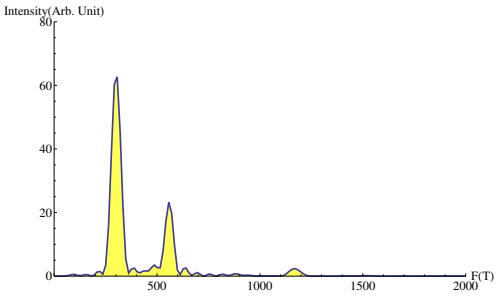

FIG. 7. Fourier transform of the oscillation spectra after a background subtraction with a cubic polynomial. $W_0 = 0.65t$, $V_c = 0.05t$, $\mu = -0.83t$, $M = 30\ a$, $N = 10^5\ a$, $\ell_D = 8\ a$, $g_V = 0.2t$. Doping is 12.46%.

V. DISCUSSION AND OUTLOOK

The complex materials physics of high temperature superconductors lead to a fairly large number of dimensionless parameters. Thus, it is not possible to frame a unique theory. Tuning these parameters can indeed lead to many different phases. However, there may be a general framework that could determine the overall picture. To be more specific, let us consider the quantum oscillation measurements that we have been discussing here.

- Are the applied magnetic fields sufficiently large to essentially destroy all traces of superconductivity and thereby reveal the underlying normal state from which superconductivity develops? While for NCCO this is clearcut because H_{c2} is less than 10T, while the quantum oscillation measurements are carried out between $30 - 65$T, far above H_{c2}. For YBCO lingering doubts remain. However, one may argue that the high field measurements are such that one may be in a vortex liquid state where the slower vortex degrees of freedom may simply act as quenched disorder to the nimble electrons. This is the picture we have adopted here.

- The emergent picture of Fermi pockets are seemingly at odds with ARPES, unless only half the pocket is visible in ARPES, as was previously argued.[28] On the other hand, reliable ARPES in YBCO is not available. For electron doped NCCO or PCCO this appears not be true.[29]

- Almost all scenarios place the observed electron pockets at the anti-nodal points in the Brillouin zone, while many other experiments would require the pseudogap to be maximum there. One may, however, question if there is only one pseudo gap.

- Quantum oscillations of R_H are easier to explain if there are at least two closed pockets in the Boltzmann picture.[6] Thus associated with the electron pocket there must be a hole pocket or vice versa. This is not a problem with NCCO, as we have shown how magnetic breakdown,[12] and a greater degree of intrinsic disorder, provides a simple resolution as to why only one pocket, in this case a small but prominent hole pocket is seen. In any case, oscillations of R_H in NCCO is yet to be measured. With respect to YBCO this becomes a serious problem. Any commensurate picture would lead to a hole pocket of frequency about twice that of the electron pocket frequency if the Luttinger sum rule is to be satisfied. Despite motivated effort no evidence in this regard has emerged. An escape from the dilemma is to propose an incommensurate picture in which the relevant electron pocket is accompanied by a much *smaller* hole pocket and some open orbits, as we have done here. In order to convincingly observe such small hole pocket, one would require extending these measurements to almost impossibly higher fields; see, however, Ref. 20.

- All oscillation measurements to date have been convincingly interpreted in terms of the Lifshitz-Kosevich theory for which the validity of Fermi liquid theory and the associated Landau levels seem to be obligatory. Why should the normal state of an under doped cuprate behave like a Fermi liquid?

- The contrast between electron and hole doped cuprates is interesting. In NCCO the crystal structure consists of a single CuO plane per unit cell, and, in contrast to YBCO, there are no complicating chains, bilayers, ortho-II potential, stripes, etc.[29] Thus, it would appear to be ideal for gleaning the mechanism of quantum oscillations. On the other hand, disorder in NCCO is significant. It is believed that well-ordered chain materials of YBCO contain much less disorder by comparison.

- In YBCO, studies involving tilted field seem to rule out triplet order parameter, hence SDW.[14,15] Moreover, from NMR measurements at high fields, there appears

to be no evidence of a static spin density wave order in YBCO.[16] Similarly there is no evidence of SDW order in fields as high as $23.2T$ in $YBa_2Cu_4O_8$[30], while quantum oscillations are clearly observed in this material.[3,4] Also no such evidence of SDW is found up to $44T$ in $Bi_2Sr_{2-x}La_xCuO_{6+\delta}$.[31] At present, results from high field NMR in NCCO does not exist, but measurements are in progress.[32] The zero field neutron scattering measurements indicate very small spin-spin correlation length in the relevant doping regime.[33] Energetically a perturbation even as large as $45T$ field is weak.[34]

- As to singlet order, relevant to quantum oscillations,[35] charge density wave is a possibility, which has recently found some support in the high field NMR measurements in YBCO.[16] But since the mechanism is helped by the oxygen chains, it is unlikely that the corresponding NMR measurements in NCCO will find such a charge order. Moreover, the observed charge order in YBCO sets in at a much lower temperature $(20-50K)$ compared to the pseudogap. Thus the charge order may be parasitic. As to singlet DDW, there are two neutron scattering measurements that seem to provide evidence for it.[36] However, these measurements have not been confirmed by further independent experiments. However, DDW order should be considerably hidden in NMR involving nuclei at high symmetry points, because the orbital currents should cancel.

As mentioned above, a mysterious feature of quantum oscillations in YBCO is the fact that only one type of Fermi pockets is observed. If two-fold commensurate density wave is the mechanism, this will violate the Luttinger sum rule.[6,37] We had previously provided an explanation of this phenomenon in terms of disorder arising from both defects and vortex scattering in the vortex liquid phase;[25] however, the arguments are not unassailable. In contrast, for NCCO, the experimental results are quite consistent with a simple theory presented previously. The present work, based on incommensurate DDW, may provide another, if not a more plausible alternative in YBCO.

The basic question as to why Fermi liquid concepts should apply remains an important unsolved mystery.[38] It is possible that if the state revealed by applying a high magnetic field has a broken symmetry with an order parameter (hence a gap), the low energy excitations will be quasiparticle-like, not a spectra with a branch cut, as in variously proposed strange metal phases.

VI. ACKNOWLEDGMENTS

We would like to thank S. Kivelson and B. Ramshaw for very helpful discussion. This work is supported by NSF under the Grant DMR-1004520.

[1] N. Doiron-Leyraud, C. Proust, D. LeBoeuf, J. Levallois, J.-B. Bonnemaison, R. Liang, D. A. Bonn, W. N. Hardy, and L. Taillefer, Nature **447**, 565 (2007).
[2] S. Chakravarty, Science **319**, 735 (2008).
[3] E. A. Yelland, J. Singleton, C. H. Mielke, N. Harrison, F. F. Balakirev, B. Dabrowski, and J. R. Cooper, Phys. Rev. Lett. **100**, 047003 (2008).
[4] A. F. Bangura, J. D. Fletcher, A. Carrington, J. Levallois, M. Nardone, B. Vignolle, P. J. Heard, N. Doiron-Leyraud, D. LeBoeuf, L. Taillefer, S. Adachi, C. Proust, and N. E. Hussey, Phys. Rev. Lett. **100**, 047004 (2008).
[5] A. J. Millis and M. R. Norman, Phys. Rev. B **76**, 220503 (2007).
[6] S. Chakravarty and H.-Y. Kee, Proc. Natl. Acad. Sci. USA **105**, 8835 (2008).
[7] I. Dimov, P. Goswami, X. Jia, and S. Chakravarty, Phys. Rev. B **78**, 134529 (2008).
[8] D. Podolsky and H.-Y. Kee, Physical Review B **78**, 224516 (2008).
[9] K.-T. Chen and P. A. Lee, Phys. Rev. B **79**, 180510 (2009).
[10] H. Yao, D.-H. Lee, and S. Kivelson, Phys. Rev. B **84**, 012507 (2011).
[11] T. Helm, M. V. Kartsovnik, M. Bartkowiak, N. Bittner, M. Lambacher, A. Erb, J. Wosnitza, and R. Gross, Phys. Rev. Lett. **103**, 157002 (2009); T. Helm, M. V. Kartsovnik, I. Sheikin, M. Bartkowiak, F. Wolff-Fabris, N. Bittner, W. Biberacher, M. Lambacher, A. Erb, J. Wosnitza, and R. Gross, *ibid*. **105**, 247002 (2010); M. V. Kartsovnik and et al., New J. Phys. **13**, 015001 (2011).
[12] J. Eun, X. Jia, and S. Chakravarty, Phys. Rev. B **82**, 094515 (2010); J. Eun and S. Chakravarty, *ibid*. **84**, 094506 (2011).
[13] L. Taillefer, Journal of Physics: Condensed Matter **21**, 164212 (2009).
[14] B. J. Ramshaw, B. Vignolle, R. Liang, W. N. Hardy, C. Proust, and D. A. Bonn, Nat. Phys. **7**, 234 (2011).
[15] S. E. Sebastian, N. Harrison, M. M. Altarawneh, F. F. Balakirev, C. H. Mielke, R. Liang, D. A. Bonn, W. N. Hardy, and G. G. Lonzarich, "Direct observation of multiple spin zeroes in the underdoped high temperature superconductor $YBa_2Cu_3O_{6+x}$," (2011), arXiv:1103.4178v1 [cond-mat].
[16] T. Wu, H. Mayaffre, S. Kramer, M. Horvatic, C. Berthier, W. Hardy, R. Liang, D. Bonn, and M.-H. Julien, Nature **477**, 191 (2011).
[17] S. Lederer and S. Kivelson, "Observable NMR signal from circulating current order in YBCO," (2011), arXiv:1112.1755.
[18] C. Nayak, Phys. Rev. B **62**, 4880 (2000).
[19] S. Chakravarty, R. B. Laughlin, D. K. Morr, and C. Nayak, Phys. Rev. B **63**, 094503 (2001).
[20] J. Singleton, C. de la Cruz, R. D. McDonald, S. Li, M. Altarawneh, P. Goddard, I. Franke, D. Rickel, C. H. Mielke, X. Yao, and P. Dai, Phys. Rev. Lett. **104**, 086403 (2010).
[21] M. A. Hossain, J. D. F. Mottershead, D. Fournier, A. Bostwick, J. L. McChesney, E. Rotenberg, R. Liang, W. N. Hardy, G. A. Sawatzky, I. S. Elfimov, D. A. Bonn, and A. Damascelli, Nat Phys **4**, 527 (2008).
[22] A. Damascelli, Z. Hussain, and Z. X. Shen, Rev. Mod. Phys. **75**, 473 (2003).

[23] E. Pavarini, I. Dasgupta, T. Saha-Dasgupta, O. Jepsen, and O. K. Andersen, Phys. Rev. Lett. **87**, 047003 (2001).
[24] Y. Sassa, M. Radovi, M. Mnsson, E. Razzoli, X. Y. Cui, S. Pailhs, S. Guerrero, M. Shi, P. R. Willmott, F. Miletto Granozio, J. Mesot, M. R. Norman, and L. Patthey, Phys. Rev. B **83**, 140511 (2011).
[25] X. Jia, P. Goswami, and S. Chakravarty, Phys. Rev. B **80**, 134503 (2009).
[26] J. L. Pichard and G. André, Europhys. Lett. **2**, 477 (1986); D. S. Fisher and P. A. Lee, Phys. Rev. B **23**, 6851 (1981).
[27] S. C. Riggs, O. Vafek, J. B. Kemper, J. Betts, A. Migliori, W. N. Hardy, R. Liang, D. A. Bonn, and G. Boebinger, Nat. Phys. **7**, 332 (2011).
[28] S. Chakravarty, C. Nayak, and S. Tewari, Phys. Rev. B **68**, 100504 (2003).
[29] N. P. Armitage, P. Fournier, and R. L. Green, Rev. Mod. Phys. **82**, 2421 (2009).
[30] G.-q. Zheng, W. G. Clark, Y. Kitaoka, K. Asayama, Y. Kodama, P. Kuhns, and W. G. Moulton, Phys. Rev. B **60**, R9947 (1999).
[31] S. Kawasaki, C. Lin, P. L. Kuhns, A. P. Reyes, and G.-q. Zheng, Phys. Rev. Lett. **105**, 137002 (2011).
[32] S. E. Brown, (2011).
[33] E. M. Motoyama, G. Yu, I. M. Vishik, O. P. Vajk, P. K. Mang, and M. Greven, Nature **445**, 186 (2007).
[34] H. K. Nguyen and S. Chakravarty, Phys. Rev. B **65**, 180519 (2002).
[35] D. Garcia-Aldea and S. Chakravarty, Phys. Rev. B **82**, 184526 (2011); M. R. Norman and J. Lin, *ibid*. **82**, 060509 (2011); R. Ramazashvili, Phys. Rev. Lett. **105**, 216404 (2011).
[36] H. A. Mook, P. Dai, S. M. Hayden, A. Hiess, J. W. Lynn, S. H. Lee, and F. Doğan, Phys. Rev. B **66**, 144513 (2002); H. A. Mook, P. Dai, S. M. Hayden, A. Hiess, S. H. Lee, and F. Doğan, *ibid*. **69**, 134509 (2004).
[37] J. M. Luttinger, Phys. Rev. **119**, 1153 (1960); A. V. Chubukov and D. K. Morr, Phys. Rep. **288**, 355 (1997); B. L. Altshuler, A. V. Chubukov, A. Dashevskii, A. M. Finkel'stein, and D. K. Morr, Europhys. Lett. **41**, 401 (1998).
[38] S. Chakravarty, Rep. Prog. Phys. **74**, 022501 (2011).

References

[1] J. Bardeen, L. Cooper, and J. Schriedffer. Theory of superconductivity. *Phys. Rev.*, 108:1175, 1957.

[2] Michael Tinkham. *Introduction to Superconductivity*. Dover, New York, USA, 1996.

[3] S. Chakravarty. Quantum oscillations and key theoretical issues in high temperature superconductors from the perspective of density waves. *Rep. Prog. Phys*, 74:022501, 2011.

[4] D. Shoenberg. *Magnetic oscillations in metals*. Cambridge University Press, Cambridge, England, 1984.

[5] T. Ando. Theory of quantum transport in a 2-dimensional electron system under magnetic fields (iv). oscillatory conductivity. *J. Phys. Soc. Japan*, 37:1233, 1974.

[6] D. S. Fisher and P. A. Lee. Relation between conductivity and transmission matrix. *Phys. Rev. B*, 23:6851, 1981.

[7] B. Kramer and A. MacKinnon. Localization: theory and experiment. *Rep. Prog. Phys*, 56:1469, 1993.

[8] B. Kramer and M. Schreiber. *in Computational Physics*. Springer, Berlin, German, 1996.

[9] T. Helm, M. V. Kartsovnik, M. Bartkowiak, N. Bittner, M. Lambacher, A. Erb, J. Wosnitza, and R. Gross. Evolution of the Fermi surface of the electron-doped high-temperature superconductor $Nd_{2-x}Ce_xCuO_4$ revealed by Shubnikov–de Haas oscillations. *Phys. Rev. Lett.*, 103(15):157002–4, 2009.

[10] T. Helm, M. Kartsovnik, I. Sheikin, M. Bartkowiak, F. Wolff-Fabris, N. Bittner, W. Biberacher, M. Lambacher, A. Erb, J. Wosnitza, and R. Gross. Magnetic breakdown in the electron-doped cuprate superconductor $nd_{2-x}ce_xcuo_4$: The reconstructed fermi surface survives in the strongly overdoped regime. *Phys. Rev. Lett.*, 105:247002, 2010.

[11] M. Kartsovnik, T. Helm, C. Putzke, F. Wolff-Fabris, I. Sheikin, S. Lepault, C. Proust, D. Vignolles, N. Bittner, W. Biberacher, A. Erb, J. Wosnitza, and R. Gross. Fermi surface of the electron-doped cuprate superconductor $nd_{2-x}ce_xcuo_4$ probed by high-field magnetotransport. *New Journal of Phys.*, 13:015001, 2011.

[12] C. Kusko, R. Markiewicz, M. Lindroos, and A. Bansil. Fermi surface evolution and collapse of the mott pseudogap in $nd2 - xce_xcuo_{4\pm\delta}$. *Phys. Rev. B*, 66:140513, 2002.

[13] Nicolas Doiron-Leyraud, Cyril Proust, David LeBoeuf, Julien Levallois, Jean-Baptiste Bonnemaison, Ruixing Liang, D. A. Bonn, W. N. Hardy, and Louis Taillefer. Quantum oscillations and the Fermi surface in an underdoped high-T_c superconductor. *Nature*, 447(7144):565–568, 2007.

[14] E. A. Yelland, J. Singleton, C. H. Mielke, N. Harrison, F. F. Balakirev, B. Dabrowski, and J. R. Cooper. Quantum oscillations in the underdoped cuprate $YBa_2Cu_4O_8$. *Phys. Rev. Lett.*, 100(4):047003–4, 2008.

[15] A. F. Bangura, J. D. Fletcher, A. Carrington, J. Levallois, M. Nardone, B. Vignolle, P. J. Heard, N. Doiron-Leyraud, D. LeBoeuf, L. Taillefer, S. Adachi, C. Proust, and N. E. Hussey. Small Fermi surface pockets in underdoped high temperature superconductors: Observation of Shubnikov–de Haas oscillations in $YBa_2Cu_4O_8$. *Phys. Rev. Lett.*, 100(4):047004–4, 2008.

[16] I. Dimov, P. Goswami, X. Jia, and S. Chakravarty. Competing order, fermi surface reconstruction, and quantum oscillations in underdoped high-temperature superconductors. *Phys. Rev. B*, 63:094503, 2001.

[17] T. Wu, H. Mayaffre, S. Kramer, M. Horvatic, C. Berthier, W. Hardy, R. Liang, D. Bonn, , and M.-H. Julien. Magnetic-field-induced charge-stripe order in the high-temperature superconductor $yba_2cu_3o_y$. *Nature*, 477:191, 2011.

[18] J. Singleton, C. de la Cruz, R. D. McDonald, S. Li, M. Altarawneh, P. Goddard, I. Franke, D. Rickel, C. H. Mielke, X. Yao, and P. Dai. Magnetic quantum oscillations in $YBa_2Cu_3O_{6.61}$ and $YBa_2Cu_3O_{6.69}$ in fields of up to 85T; patching the hole in the roof of the superconducting dome. *Phys. Rev. Lett.*, 104:086403, 2010.

[19] Andrew J. Millis and M. R. Norman. Antiphase stripe order as the origin of electron pockets observed in 1/8-hole-doped cuprates. *Phys. Rev. B*, 76(22):220503–4, 2007.